ANALYSIS OF ADVANCED ACTINIDE-FUELED ENERGY SYSTEMS FOR DEEP SPACE PROPULSION APPLICATIONS

A Thesis

by

TROY LAMAR GUY

Submitted to the Office of Graduate Studies of
Texas A&M University
in partial fulfillment of the requirements for the degree of

MASTER OF SCIENCE

December 2009

Major Subject: Nuclear Engineering

ANALYSIS OF ADVANCED ACTINIDE-FUELED ENERGY SYSTEMS FOR DEEP SPACE PROPULSION APPLICATIONS

A Thesis

by

TROY LAMAR GUY

Submitted to the Office of Graduate Studies of
Texas A&M University
in partial fulfillment of the requirements for the degree of

MASTER OF SCIENCE

Approved by:

Chair of Committee,	Pavel V. Tsvetkov
Committee Members,	Shannon M. Bragg-Sitton
	Nicholas B. Suntzeff
Head of Department,	Raymond J. Juzaitis

December 2009

Major Subject: Nuclear Engineering

ABSTRACT

Analysis of Advanced Actinide-Fueled Energy Systems for Deep Space Propulsion Applications. (December 2009)

Troy Lamar Guy, B.S. University of Houston

Chair of Advisory Committee: Dr. Pavel V. Tsvetkov

The present study is focused on evaluating higher actinides beyond uranium that are capable of supporting power and propulsion requirements in robotic deep space and interstellar exploration. The central technology in this thesis is based on utilizing advanced actinides for direct fission fragment energy conversion coupled with magnetic collimation. Critical fission configurations are explored which are based on fission fragment energy conversion utilizing a nano-scale layer of the metastable isotope ^{242m}Am coated on carbon fibers. A 3-D computational model of the reactor core is developed and neutron properties are presented. Fission neutron yield, exceptionally high thermal fission cross sections, high fission fragment kinetic energy and relatively low radiological emission properties are identified as promising features of ^{242m}Am as a fission fragment source. The isotopes ^{249}Cf and ^{251}Cf are found to be promising candidates for future studies. Conceptual system integration, deep space mission applicability and recommendations for future experimental development are introduced.

ACKNOWLEDGEMENTS

The task of thanking everyone who assisted me in completing this thesis is a humbling task. Pavel Tsvetkov, my committee chair and friend, has been incredibly patient, always answering late night questions, guiding me when concepts were fuzzy and always being available to me despite his own schedule. I am grateful to Shannon Bragg-Sitton and Nick Suntzeff for serving on my thesis committee and providing invaluable comments throughout this work.

I would like to recognize my employer, Lockheed Martin, for supporting me in professional and academic life. I recognize Olivia Fuentes, for without her constant support this thesis would not be possible.

My parents, Burt and Linda Guy, have played an unbelievably important support role in this thesis. I'm thankful for their emotional and encouraging support to finish this thesis. Thank you.

My mother and father-in-law have played a wonderful role in this thesis by always being supportive, providing comments and helping in multiple ways.

My wife, Lisa, has been a rock during times of stress and when research drew me away from family. I am thankful for her love, her faithfulness and her deep compassion for understanding while I spent hours poring over computational nuclear code data. My daughter, Hannah, is always available for a good hug and a smile when research seemed to be going slow. Cameron, my son, is another blessing of support, always jumping on me with love when coming home late from school. I am so very thankful for my family.

Thanks to the entire Nuclear Engineering faculty, staff and friends at Texas A&M University for instilling in me the freedom to study a highly unique field with immense rewards and the best nuclear experimental research facilities in the world.

Juggling between family, academics, research and professional work has been a complicated mission. I want to thank God, whose real and constant hand in my life has brought me through wonderful experiences.

NOMENCLATURE

ASRG	Advanced Stirling Radioisotope Generator
AU	Astronomical Unit
BOM	Beginning of Mission
COTS	Commercial Off The Shelf
DEC	Direct Energy Conversion
DFFEC	Direct Fission Fragment Energy Conversion
DOE	Department of Energy
ENDF	Evaluated Nuclear Data Files
EOM	End of Mission
FF	Fission Fragment
FFMCR	Fission Fragment Magnetic Collimator Reactor
JANIS	Java-based Nuclear Information Software
JIMO	Jupiter Icy Moons Orbiter
LWR	Light Water Reactor
NASA	National Aeronautics and Space Administration
NDDEC	Nuclear Driven Direct Energy Conversion
NEP	Nuclear Electric Propulsion
NERI	Nuclear Energy Research Initiative
NERVA	Nuclear Engine for Rocket Vehicle Application
NTP	Nuclear Thermal Propulsion

RTG	Radioisotope Thermoelectric Generator
SCALE	Standardized Computer Analysis for Licensing Evaluation
SNAP	Systems for Nuclear Auxiliary Power
SRIM	Stopping and Range of Ions in Matter
STK	Satellite Tool Kit
TFE	Thermionic Fuel Elements
TRL	Technology Readiness Level

TABLE OF CONTENTS

CHAPTER Page

LIST OF FIGURES

Page

LIST OF TABLES

Page

CHAPTER I

INTRODUCTION

Deep space exploration has captured the imagination of the human spirit for thousands of years. Advanced deep space and interstellar propulsion concepts are critical to advancing future exploration, both locally in our solar system and in exosolar applications. Investigation of interstellar space regions have yet to be achieved beyond 200 astronomical units (AU), where one AU is the average distance between Earth and the Sun (approximately 150 million km). Pristine interstellar matter is expected to exist in this region. Advanced missions currently without a viable, robust mechanism for exploration include: Stellar probes, interstellar probes, Kuiper belt rendezvous vehicles, Oort cloud explorers and nearest-star targets. Outer edge solar system planets, atmospheres and planetary moon systems may hold insights into the physics of the early universe, yet they too have been largely unexplored. Terrestrial visits to Mars polar caps and Jupiter's icy moon oceans have been identified as future missions requiring advanced power and propulsion techniques. Despite overwhelming scientific interest and over 50 years of research, a robust mechanism for rapid space and interstellar exploration remains elusive.

Propulsion and power technology applicable to deep space missions has generally fallen into four classes: chemical, fission, fusion, and exotic physics-based concepts.

This thesis follows the style of *Nuclear Science and Engineering.*

Despite persistent research in novel high-energy molecular chemical fuels and advanced bipropellant rocket engine concepts [1], chemical propulsion systems are limited to about 480 seconds of specific impulse, a value much too low to successfully meet deep space propulsion requirements. Owing to relatively low power per unit mass of ejected matter ratios and inherently limited chemical reaction energetics, chemical propulsion systems appear inadequate as primary fuel sources for interstellar or extended solar system edge missions.

Fission reactors have long been proposed to address power and propulsion requirements. Essentially all solid, liquid and gas fission reactors fundamentally operate by converting kinetic energy from fission reactions into heat through a working fluid. This thesis will focus on a concept that utilizes the fission process but is fundamentally different than thermal or fast spectrum fission reactors and may offer a viable solution to stringent propulsion and power requirements related to deep space.

Nuclear fusion holds tremendous potential for future space exploration initiatives. Inertial confinement, magnetic confinement, gas dynamic and magnetized target fusion concepts have been proposed [2]. Specific impulses on the order of 10^3 seconds are theoretically possible. Unfortunately, nuclear fusion ignition, confinement of hot dense plasma and extreme heat management continue to be enormous obstacles for even mid-term fusion-based propulsion and power systems.

Exotic physics-based concepts are varied in nature. Antimatter, solar sails, magnetic sails, beamed energy and fusion ramjets have been proposed for advanced propulsion. Limited technological developments appear to have restricted near-term

deployment in space propulsion or power applications. This is evident in perhaps the most exciting exotic space propulsion candidate, antimatter. Matter-antimatter has excellent atomic reaction properties including converted mass factions of 1.0 and energy releases of $9x10^{16}$ joules per kilogram in the case of proton-antiproton reactions (as compared to $2x10^{8}$ joules per kilogram for atomic hydrogen and $3.4x10^{14}$ joules per kilogram for Deuterium-Deuterium or Deterium-Helium-3 fusion fuels) [3]. Antimatter candidates have theoretical specific impulses of 10^{5}-10^{6} seconds. Despite these highly attractive theoretical merits, antimatter candidate fuels have significant technological barriers such as the production and storage of antimatter. In addition, antimatter must be directed for thrust, a grand challenge yet to be mastered.

I.A. Review of Space Nuclear Programs

Propulsion and power systems developed for space exploration have historically focused on developing three types of systems: nuclear thermal propulsion (NTP), nuclear electric propulsion (NEP) and radioisotope thermoelectric generators (RTGs). NTP systems generate heat in a reactor which heats gas to very high temperatures. The heated gas expands and is ejected through a nozzle to create power and thrust. NEP systems use heat-to-electrical energy conversion mechanisms for generating electric power from heat provided by the reactor core. In general, NTP produces medium-to-high thrust with Isp levels on the order of 1000 s, while NEP systems typically provide higher Isp but much lower thrust levels [4]. Radioisotope power systems benefit from the direct

radioactive decay of isotopes to generate electric power, but require a thermoelectric energy conversion process. Heat is converted to electricity using thermocouples.

I.A.1. Nuclear Thermal Propulsion

In the 1950's a study was initiated by the United States Air Force with the goal of designing and testing nuclear rockets [5]. The ROVER program was created as a succession of nuclear reactor tests. A major focus of this program was to demonstrate that a nuclear reactor could be used to heat a gas to very high temperatures, which would then expand and be directed through a nozzle to create thrust [5]. In 1959 a series of reactors under the ROVER program were developed known as the Kiwi series. Highlights of this series include the Kiwi-A, Kiwi-B and Kiwi-B4E reactors. Kiwi-A utilized gaseous hydrogen for propellant, while Kiwi-B used liquid hydrogen and was designed to be 10-times the power of Kiwi-A. Kiwi-A and Kiwi-B successfully proved that a nuclear reactor could operate with high temperature fuels and utilize hydrogen (gaseous and liquid). The Kiwi series of tests ended with Kiwi-B4E. A second series of reactors developed in the 1960's under the ROVER program were known as the Phoebus series. The Phoebus 1 reactor was designed for up to 2.2×10^5 N of thrust and 1500 MW power. Phoebus 2A was designed for up to 5000 MW of power and up to 1.1×10^6 N of thrust. Phoebus 2A is the most powerful reactor ever built with actual record power and thrust levels of 4100 MW and 9.3×10^5 N of power and thrust, respectively [6]. In addition to the Kiwi and Phoebus series of reactors, two other reactors under the

NERVA (Nuclear Engine for Rocket Vehicle Application) program were the Pewee and Nuclear Furnace. Pewee was developed to demonstrate nuclear propulsion in space. The fuel selected for the Pewee reactor was niobium carbide (NbC) zirconium carbide (ZrC) [5]. In 1972, the Nuclear Furnace reactor was successful in demonstrating carbide-graphite composite fuel with a zirconium-carbide outer fuel layer that could be used as fuel [5]. The ROVER/NERVA program successfully demonstrated that graphite reactors and liquid hydrogen propellants could be used for space propulsion and power, with thrust capabilities up to 1.1×10^6 N and specific impulse of up to 850 seconds [7]. However, NTP research has been minimal since these periods.

I.A.2. Nuclear Electric Power

In the 1950's a study was initiated under the Atomic Energy Commission which developed a series of reactors. This series was termed the Systems for Nuclear Auxiliary Power (SNAP) program. While multiple reactors were researched and developed (SNAP-series), the SNAP-10A reactor, flown in 1965, became the only United States fission reactor ever to be launched into space. The core consisted of enriched uranium-zirconium-hydride (U-ZrH) fuel, a beryllium (Be) reflector, a NaK coolant loop and a 1° per 300 second rotating control drum [8]. After reaching orbit and operating for 43 days, the SNAP-10A was shut down due to a failure in a non-nuclear regulator component. Currently, the SNAP-10A is in a 4000 year parking orbit [8].

In the former USSR, more than 30 space power reactors were built and flown in space between 1970-1988. For example, the BUK thermoelectric uranium-molybdenum (U-Mo) fueled, sodium-potassium (NaK) cooled reactor was designed to provide power for low altitude spacecraft in support of marine radar observations [9]. The BUK core consisted of 37 fuel rods and operated with a fast neutron spectrum. In 1987 the Russian TOPAZ reactor operated in space for 142 days and consisted of 79 thermionic fuel elements (TFE's) [9] and a NaK coolant system. Two flights of the TOPAZ reactor were conducted. TOPAZ-1 was launched in 1987 and operated for 142 days. TOPAZ-II was launched in 1987 and operated for 342 days.

Project Prometheus, a program initiated in 2003 by NASA, was established to explore deep space with long duration, highly reliable technology. Under the Prometheus charter, the Jupiter Icy Moons Orbiter (JIMO) project was conceived to explore three Jovian icy moons: Callisto, Ganymede and Europa. These moons were selected due to their apparent water, chemical, energy and potential life supporting features [10]. The selected reactor would operate for 10-15 years and provide approximately 200 kW_e of electric power [11]. Five reactor designs were studied as part of a selection process: low temperature liquid sodium reactor (LTLSR), liquid lithium cooled reactor with thermoelectric (TE) energy conversion, liquid lithium cooled reactor with Brayton energy conversion, gas reactor with Brayton energy conversion and a heat pipe cooled reactor with Brayton energy conversion. A gas reactor, with Brayton energy conversion, was chosen as the highest potential to support the JIMO deep space mission.

I.A.3. Radioisotope Power

Radioisotope thermoelectric generators (RTG) function by the radioactive decay process of nuclear material, such as Plutonium-238 (Pu-238), Strontium-90 (Sr-90), Curium-244 (Cu-244) or Cobalt-60 (Co-60). Many isotopes have been considered and are evaluated as potential power sources based, in part, on mechanical (form factor, melting point, production, energy density) and nuclear (half-life, energy density per unit density, decay modes, decay energy, specific power and density) properties. Heat is produced by radioactive decay and then converted to electric power by a thermoelectric generator, which is a direct energy conversion process based on the Seebeck Effect.

In 1961, the first United States RTG was launched with one radioisotope source to produce a power of 2.7 W_e [12]. The Transit 4A spacecraft successfully reached orbit and was used for naval space navigation missions. RTG's have provided power for extended duration spacecraft missions over the past 40 years, including Apollo (moon mission), Viking (Mars mission), Voyager (outer planets and solar system edge missions), Galileo (Jupiter mission), Cassini (Saturn mission) and Pluto New Horizons (Pluto mission) [13]. In total, there have been over 45 RTGs developed and operated by the US for space power [14]. Early RTG spacecraft operated with system efficiencies around 6%. An advanced version of the RTG, termed the Advanced Stirling Radioisotope Generator (ASRG) is being considered which is expected to increase efficiency and reduce the required amount of Pu-238 carried into space, with a predicted

performance of up to 155 W_e and efficiency near 30% [15]. A third type of radioisotope generator has been proposed. The Multi-Mission Radioisotope Thermoelectric Generator (MMRTG) is under development by the Department of Energy (DOE) and the National Aeronautics and Space Administration (NASA) and is expected to provide 2000 W of thermal power using plutonium dioxide fuel. This design will support a Mars surface laboratory, operating both in space and in the Martian atmosphere [16].

I.B. Reliability-Demanding Applications and Deep Space Missions

Deep space environments are often harsh and present significant challenges to instrumentation, components, spacecraft and people. A brief summary of conditions where power and propulsion sources must perform with a high degree of reliability is discussed below.

Earth's moon will complete one full cycle every 29.53 days, creating extended cold temperatures during lunar night. Temperature can range from 403 K to pre-dawn temperatures of 93 K [17]. The moon's ultra thin atmosphere creates a dark sky during most of the lunar day. Thus, a highly reliable power source must be available for long-term exploration and human habitation. In addition, robust energy systems will enable in- depth terrestrial surveys of the far side and poles of the Moon.

At a distance of 1.524 AU, Mars has seasonal weather patterns, which give rise to temperatures between 133 K and 294 K. Weather patterns observed from the Viking Lander observed daily temperature fluctuations of 315 K [17]. In addition, temperatures

have been found to change 277 K within minutes. Dust storms have been measured to travel up to 0.028 km/s, which often distribute dust over the majority of Mars' atmosphere [17]. Solar energy flux is reduced by a half at Mars (relative to Earth) and dust storms can further reduce solar flux by up to 99% [17]. Exploration of potential trapped H_20 on Mars polar caps will require reliable power sources for transport vehicles, drilling platforms, autonomous boring machines and supporting bases, seismic measuring stations spread across planetary surfaces and atmospheric-based satellite vehicles.

In the interest of searching for pre-biotic chemistry, space exploration to the Jovian moon system has been proposed. Europa, Io, Ganymede and Callisto are planet-sized satellites of Jupiter [10]. Some of these moons are thought to contain ice or liquid water. In particular, Europa is predicted to contain oceans of liquid below its icy surface. Europa's ocean seafloors are thought to contain undersea volcanoes, a potential source of energy [10]. Probes designed to dive into sub-surface regions require critical onboard instruments to function undersea and must be driven by robust power or propulsion sources.

The Alpha Centauri star system, the closest star to Earth except the sun, is located at 200,000 AU. Proxima Centauri, one of three stars in the Alpha Centari system is the focus of advanced interstellar propulsion concepts with speculation of the existence of exoplanets. Proxima Centauri is a prohibitive destination with current state-of-the-art propulsion and power sources. For example, advanced chemical systems propelling a small robotic probe to Alpha Centari at a theoretical maximum speed of

0.001c (where c is the speed of light) would take approximately 4000 years [10]. Conversely, a robotic probe propelled to 0.1c would take 40 years. As pointed out by [10], data could be returned at light speed to Earth in 4 years after arrival. Additionally, a star observer system outside 200 AU could return images and information about Earth's solar system never observed before. Interstellar mission requirements force high reliability constraints on power sources, which will require many years of constant operation.

I.C. Nuclear-Driven Direct Energy Converters

In conventional nuclear reactors, fission energy is harnessed from a working fluid. Nuclear fission releases a distribution of particles and corresponding energies as shown in Table 1 [18].

Table 1. Component Energies in Neutron-induced Fission of ^{235}U

Energy Release in Fission, by component	**Energy (MeV)**	**Fraction (%)**
▪ Kinetic Energy of Fission Fragments (FF)	168	81.16
▪ Kinetic Energy of Fission Neutrons	5	2.42
▪ Energy of Prompt γ-rays	7	3.38
▪ Total Energy of β-particles	8	3.86
▪ Energy of Delayed γ-rays	7	3.38
▪ Energy of Neutrinos	12	5.80
Total Energy released per Nuclear Fission Event	207	100.00

The largest fraction (81.16%) of energy released in the fission process goes to the kinetic energy of FFs. FF particles from the fission process dissipate particle kinetic energy into heat, which is removed from the reactor core by a coolant such as sodium, carbon dioxide or helium. The heat removed is then used to produce energy through electromechanical energy conversion, a process subject to Carnot efficiency limitations [19]. In nuclear-driven direct energy conversion (NDDEC) FF kinetic energy is collected before fragment particles are turned into heat. In NDDEC intermediate energy conversion stages are negated and vast increases in efficiency are possible. Figure 1 shows the difference between conventional nuclear power and the FFDEC concept.

The fundamental concept of producing electric power from charged particles via nuclear reactions was proposed by H. G. C. Moseley and J. Harling in 1913 [19]. In these experiments, it was shown that charged particles could experimentally be utilized for creating high voltage. Direct fission fragment energy conversion (DFFEC) is the general process by which charged particles generated from nuclear fission are collected and directly used for energy generation or propulsion. Early studies of the DEC concept utilizing kinetic energy from FFs were initially proposed by E. P. Wigner in 1944 [4]. In 1957, G. M. Safonov performed the first theoretical study [20]. Experiments validated the basic physics of the concept, but a variety of technical challenges limited the observed efficiencies.

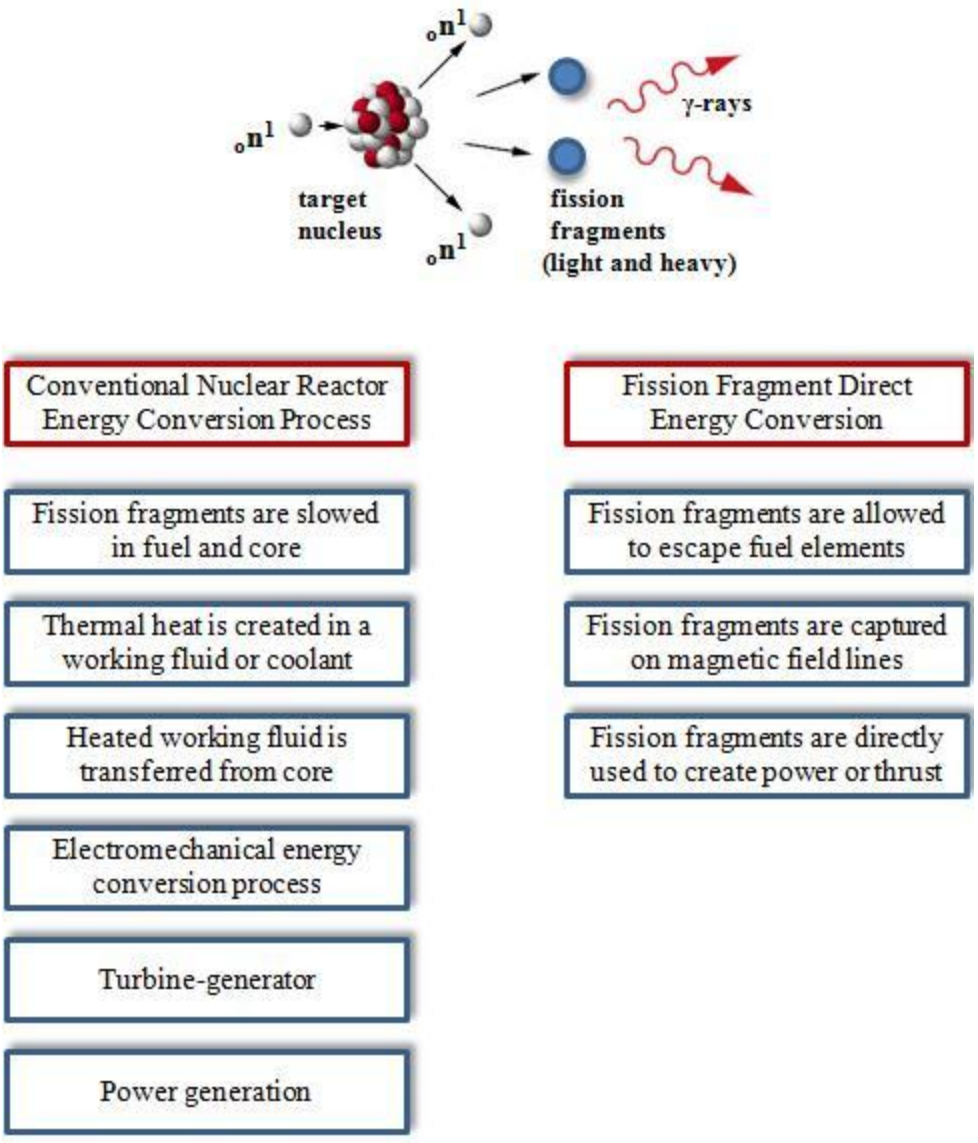

Figure 1. Conventional Nuclear Reactor and Direct Energy Conversion Processes

In addition, further studies were conducted by Chaplin [21] in which the core was in a vacuum and fissile material was inserted in the reactor core on very thin diameter fibers.

Previous work by Ronen [22] calculated the minimal fuel element thickness and the energy of the fission products emerging from these fuel elements, an element central to this thesis. It was found that it is possible to design a nuclear reactor with a cylindrical fuel element with a thickness of less than 1 μm of ^{242m}Am. In such a fuel element, 90% of the fission products can escape [22]. Further, Ronen showed that relatively low enrichments of ^{242m}Am are enough to assure nuclear criticality. This is a useful benchmark to the current thesis.

In recent studies, as part of the United States Department of Energy Nuclear Energy Research Initiative Direct Energy Conversion (DOE NERI DEC) Project, the fission fragment magnetic collimator reactor (FFMCR) concept was identified as a promising technological concept for planetary power and interstellar propulsion applications [23]. In the proposed concept, FFs exit the fuel element and are then directed out of the reactor core and through magnetic collimators by an external magnetic field to direct collectors located outside of the reactor core. This approach has the advantage of separating (in space) the generation and collection of FFs. In addition, achieving and maintaining criticality of the neutron chain reaction is easier for the FFMCR concept, as the metallic collection components can be located outside the nuclear reactor core. A feasibility study of this concept has been completed in which the basic power source is the kinetic energy of FFs that escape from a very thin fuel layer. The reactor core consists of a lattice of fuel-coated nano or micro-sized fibers utilizing graphite. After FFs exit the fuel element, they are captured on magnetic field lines and are directed out of the core and through magnetic collimators to produce thrust for space

propulsion, electricity or to be used for a variety of applications. In previously proposed concepts, the basic reactor fuel is a pure ^{242m}Am fuel layer coated on graphite fiber rods.

The FFMCR concept provides distinct fuel advantages for deep space, high-reliability applications. Some advantages include [24]:

1. Elimination of thermal-to-electric energy conversion stages
2. Very high efficiency
3. Very high specific impulse
4. Long-term operational capability
5. Reactor core with no moving parts
6. Low fuel inventory
7. Reduced Beginning of Mission (BOM) mass and volume
8. Propellant is not required
9. Significantly shorter probe transient times

I.D. Objectives of This Thesis

The focus of this thesis is the physics of advanced ^{242m}Am systems, higher actinide fuels, and a search for mixed-composition fuels and reactor fuel choices for advanced energy sources, with applications to deep space power and propulsion. Specifically, the first objective of this research proposal is to search for and analyze high neutron yield compositions of higher actinide elements. Fuel layers are coated on very thin rods, potentially including novel carbon nano-tube fiber rods. Fuel layers determine

the fundamental performance capabilities of the FFMCR and identification of critical nuclear fuel properties will allow narrowed optimization of system performance. A spectrum of fuel mixtures will be considered including Curium, Californium, Uranium, Plutonium, Neptunium and other higher actinides. A determination of optimal fuel layer compositions and geometry to produce the highest neutron yield will be reported.

A second objective of this thesis is to search for actinide fuel mixtures which produce high fission fragment production rates using ^{242m}Am as the major component. High thermal fission cross sections are characteristic of ^{242m}Am fuel. Fission fragment ions must be produced with high efficiency in mixed fuels containing ^{242m}Am to ultimately translate into thrust. This thesis will study fission fragment particle production resulting from various combinations of isotopic concentrations and geometries.

A third objective of this work is to examine whole reactor core configurations for criticality, efficiency and performance. The FFMCR core must be configured in such a way as to increase overall efficiency, power and thrust. For example, decreasing the core fuel layer thickness using nano particle substrate layers may decrease weight and increase compactness. Implementation of ^{242m}Am-based mixed oxide fuel layers doped with select isotopes may increase neutron production rates. In deep space, the ability for the reactor core to have dual function as propulsion and power may be critical. This thesis will model and analyze complete FFMCR cores to determine criticality and reactor performance characteristics as applicable to deep space exploration.

CHAPTER II

PROPERTIES OF HIGH NEUTRON YIELD COMPOSITIONS

Current concepts for extended deep space power sources are based on plutonium or uranium actinides. For example, the NASA Advanced Stirling Radioisotope Generator (ASRG) is expected to use a plutonium dioxide (PuO_2) fuel to heat Stirling converters and the Lunar Surface Fission Power (LSFP) source is expected to utilize uranium-based fuels such as uranium dioxide (UO_2) or uranium zirconium hydride (UZrH) [25]. Uranium and plutonium, the most commonly proposed energy sources for space nuclear power, will serve as baseline reference actinides for comparison and analysis against higher actinides.

Fuel for the FFMRC concept should have a half-life long enough to continually produce power over all mission phases. In addition, the fuel should be able to produce optimal power to preclude having thousands of years of life that require extraneous and costly attention beyond the end-of-mission (EOM) timeline. Essentially, an ideal energy source would have a half-life to cover the mission and then safely decay within a reasonable timeframe after the EOM has been closed.

In practical spacecraft development design, the specific activity of select nuclides should be kept as low as possible while maintaining the required power requirements from decay. Nuclides that decay and emit strong radiation fields will pose hazards to spacecraft equipment, scientific payloads and personnel. Advanced actinides for the FFMCR should have minimal radiological activity.

Specific power, the power produced per time and mass, is an important factor in determining heat shield and material requirements. Ideally, specific power should be kept as low as possible to create a technically viable space probe utilizing selected nuclides. If a nuclide exhibits a very high specific power, material margins may become serious limitations to the usefulness of the select actinide as a fuel candidate.

Neutron induced fission is the process by which the FFMCR will be started. However, when bombarding target nuclei, the probability of interaction between the projectile and target nucleus is a quantum mechanical statistical process. In other words, there is no guarantee that a neutron projected at a target nuclei will produce a desired nuclear reaction. The successful higher actinide isotope will have a high thermal neutron cross section and, for purposes of this thesis, have a higher thermal neutron fission cross section relative to baseline actinides. The probability of fission should be maximized.

In the evaluation of nuclear reactor core performance, neutron production and absorption parameters must be considered per actinide isotope. Neutrons are released during fission, with some captured by absorption reactions with surrounding nuclei. A measurement of a nuclide's ability to produce neutrons will determine the ability to create and sustain a neutron-nucleus chain reaction and ultimately the ability of the nuclide to produce energy and power. For purposes of this thesis, the desire is to identify a nuclide which will produce more neutrons than are lost relative to baseline actinides listed in Table 2.

Table 2. Baseline and Selected Candidate Higher Actinides

Baseline Actinides:	**Isotopes**
Uranium	^{235}U
Plutonium	^{238}Pu, ^{239}Pu, ^{241}Pu
Selected Actinides:	
Uranium	^{232}U
Americium	^{241}Am, ^{242m}Am
Curium	^{243}Cm, ^{244}Cm
Californium	^{249}Cf, ^{251}Cf

For deep space power to be viable, robust and effective candidate isotopes must inherently contain suitable parameters. Candidate isotopes reviewed in this thesis are analyzed according to the metrics in Table 3.

Table 3. Metric for Determining Nuclide Viability for FF Reactor Core

Property	**Metric**
$T_{1/2}$: Half-Life	18 - 900 years
A: Specific Activity	< 50 curies per gram
P: Specific Power	< 1 watt per gram
η: Neutron production	> 2.6 neutrons per neutron absorbed
σ_F: Fission Cross Section	> U, Pu baseline actinides
ff_{KE}: FF Kinetic Energy	> U, Pu baseline actinides
γ-ray: Prompt γ-ray radiation	< U, Pu baseline actinides
Φ: Energy/Charge ratio	< 5 MV stopping power

II.A. Nuclear Physics of Higher Actinides

Isotopes of Actinium through Lawrencium were assessed according to half-life for initial inclusion or exclusion in this thesis. The initial matrix criterion for acceptability was that the actinide isotope should have a half-life between 18 to 900 years. It is recognized that some isotopes on the lower range of this spectrum may not provide optimal mission timeline power or propulsion sources, but were included for completeness and comparison. Actinides such as Einsteinium, Fermium and Mendelevium were found to have half-lives too short for additional consideration as long-term energy sources. The longest lived isotopes of these actinides are shown in Figure 2.

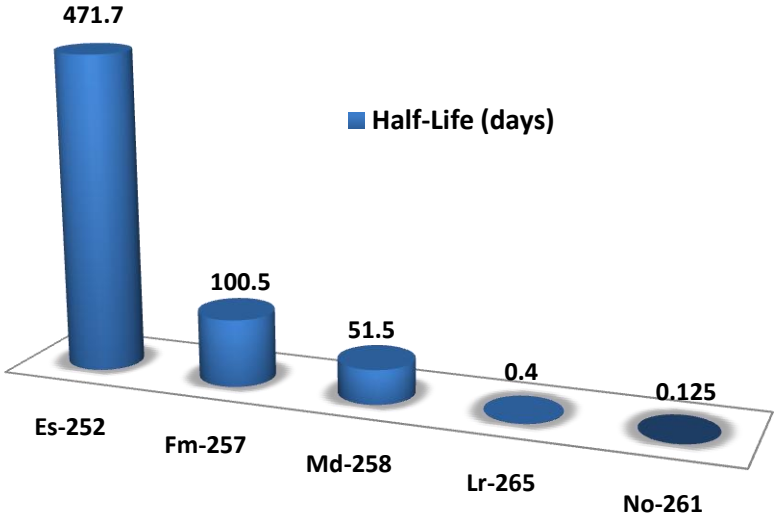

Figure 2. Longest Lived Isotopes of Einsteinium through Lawrencium

Isotopes with a short half-life may be useful for limited duration applications, but are less useful for deep space exploration due to the amount of fuel required to provide energy over a longer period of time. Isotopes with half-life between 18 to 900 years are listed in Table 4. Associated decay constants and specific activities are given. Baseline Uranium and Plutonium isotopes are included for comparison.

Table 4. Isotope Properties

Isotope	**Half-Life, $T_{1/2}$ [yr]**	**Decay Constant, λ [yr^{-1}]**	**Specific Activity, Ā [Ci/g]**
^{232}U	68.9	0.01006	22
^{235}U	704×10^{6}	9.8×10^{-10}	2.2×10^{-6}
^{238}Pu	87.7	0.00790	17
^{239}Pu	24×10^{3}	2.8×10^{-05}	6.3×10^{-2}
^{241}Pu	14.35	0.04830	100
^{241}Am	432.2	0.00160	3.5
^{242m}Am	141	0.00491	9.8
^{243}Cm	29.1	0.02381	52
^{244}Cm	18.1	0.03829	82
^{249}Cf	351	0.00197	4.1
^{251}Cf	900	0.00077	1.6

Fission reaction cross sections are critical to evaluating potential fuel candidates for the FF reactor concept. In order to produce FF particles, a given fuel must fission with a high rate of probability, which is dependent on the energy of incident neutrons and target nuclei. The Java-based Nuclear Information Software (JANIS) program was used to prepare fission cross section data.

For neutron induced reactions between 10^{-5} eV and 20 MeV, isotopes in Table 4 were plotted (see Figure 3) utilizing ENDF/B-IV evaluated nuclear data sets [26]. The three actinides having the highest fission cross sections in the thermal region are ^{242m}Am, ^{251}Cf and ^{249}Cf. Actinides with the lowest thermal spectrum fission cross sections are ^{238}Pu, ^{241}Am and ^{244}Cm.

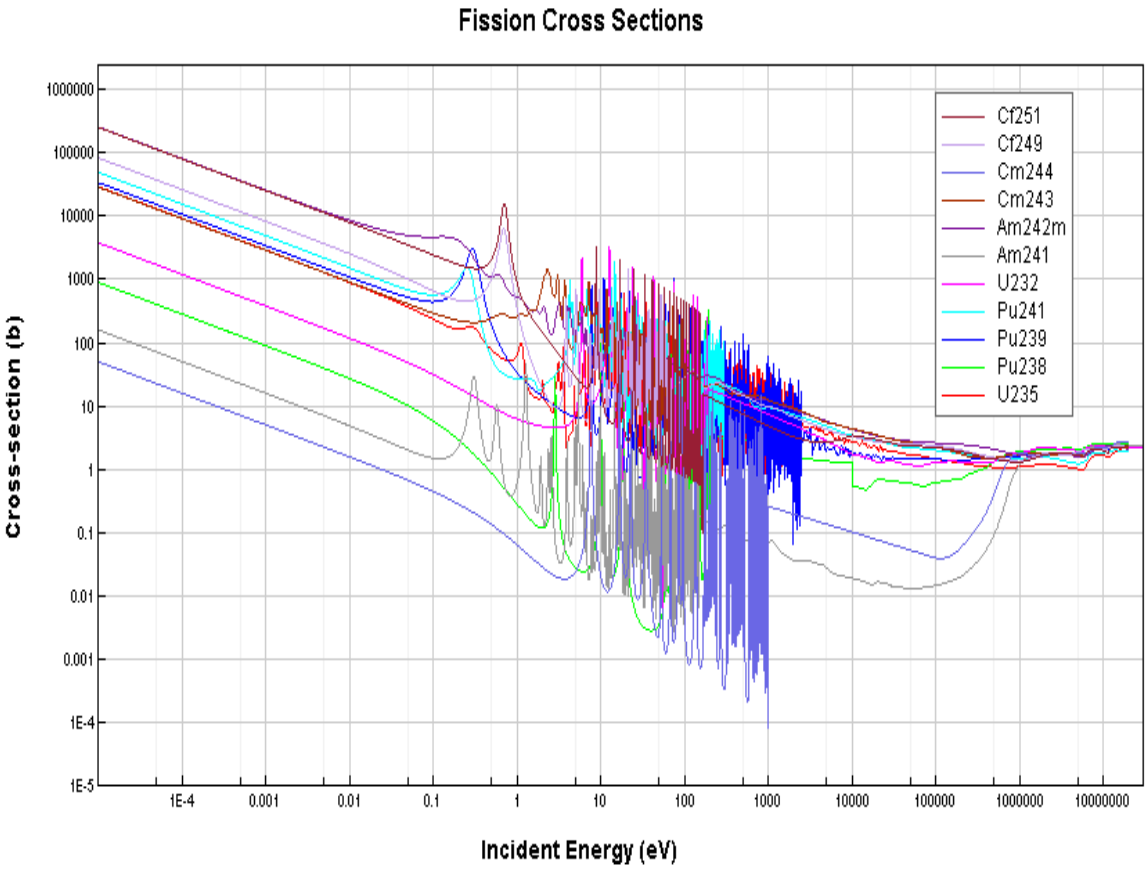

Figure 3. Fission Cross Sections from 10^{-5} eV to 10 MeV

It is observed that ^{242m}Am has a significantly higher fission cross section compared to ^{235}U and ^{239}Pu in the thermal neutron region. Baseline isotope fission cross sections are highlighted (dashed lines) and compared to higher actinide isotopes in Figure 4.

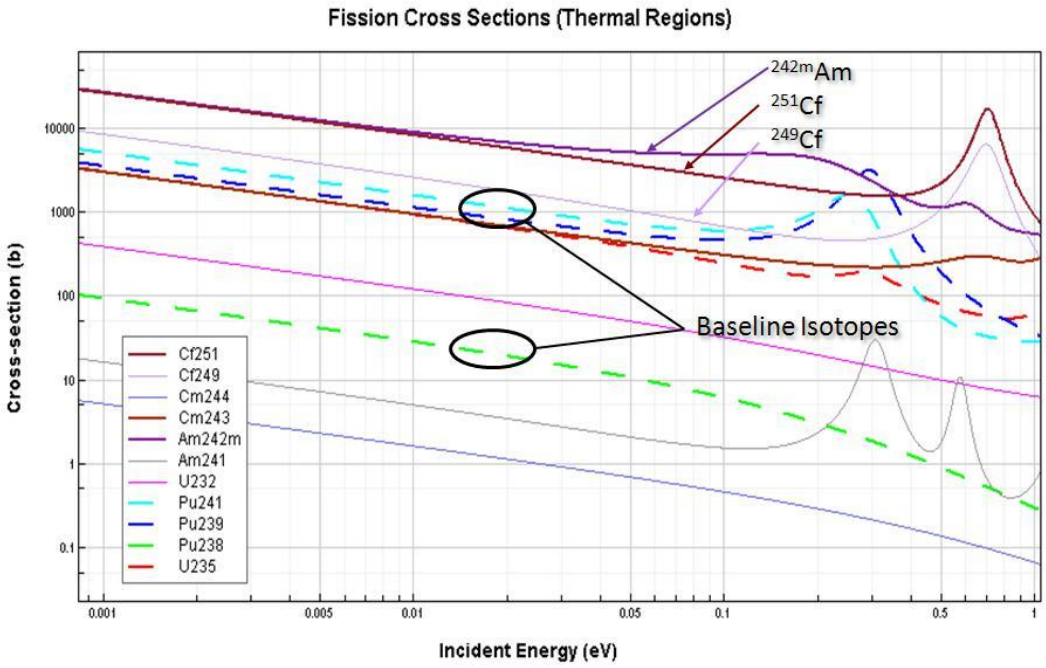

Figure 4. Fission Cross Sections from 10^{-4} eV to 1 eV

The number of neutrons created from fission per neutron absorbed, η, can be computed according to equation (1) for pure isotopes where ν is the average number of neutrons (prompt and delayed) released per fission, $\sigma_{fission}$ is the microscopic fission cross section and $\sigma_{capture}$ is the microscope capture cross section.

$$\eta = \nu \frac{\sigma_{fission}}{\sigma_{capture} + \sigma_{fission}} \quad (1)$$

To determine the number of neutrons produced per neutron absorbed, equation (1) was plotted as a function of energy as shown in Figure 5.

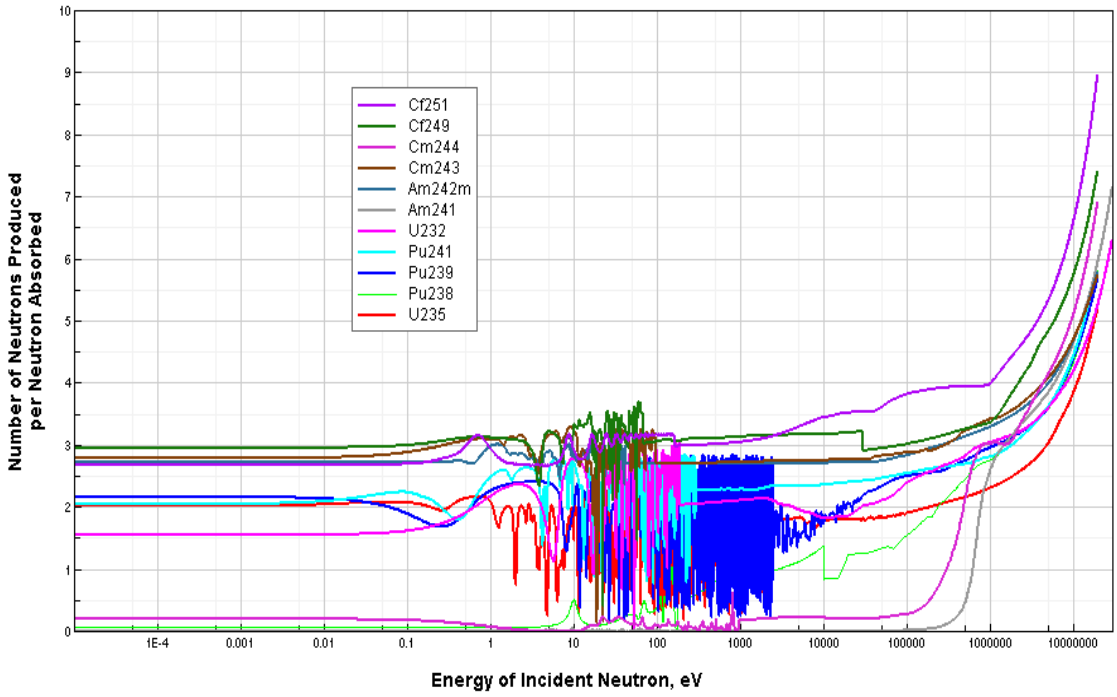

Figure 5. Number of Neutrons Produced per Neutron Absorbed (η)

Analysis of the data shows that for thermal spectrum neutron reactions, ^{249}Cf, ^{243}Cm and ^{242m}Am produce the highest η. Conversely, ^{241}Am, ^{238}Pu and ^{244}Cm appear to produce less than unity η in the thermal neutron spectrum. In the fast fission spectrum, the highest η produced occurs from the ^{251}Cf isotope and the lowest η

produced is from ^{235}U; η above approximately 10^6 eV grows exponentially with incident neutron energy. For clarity, the thermal spectrum is shown in Figure 6.

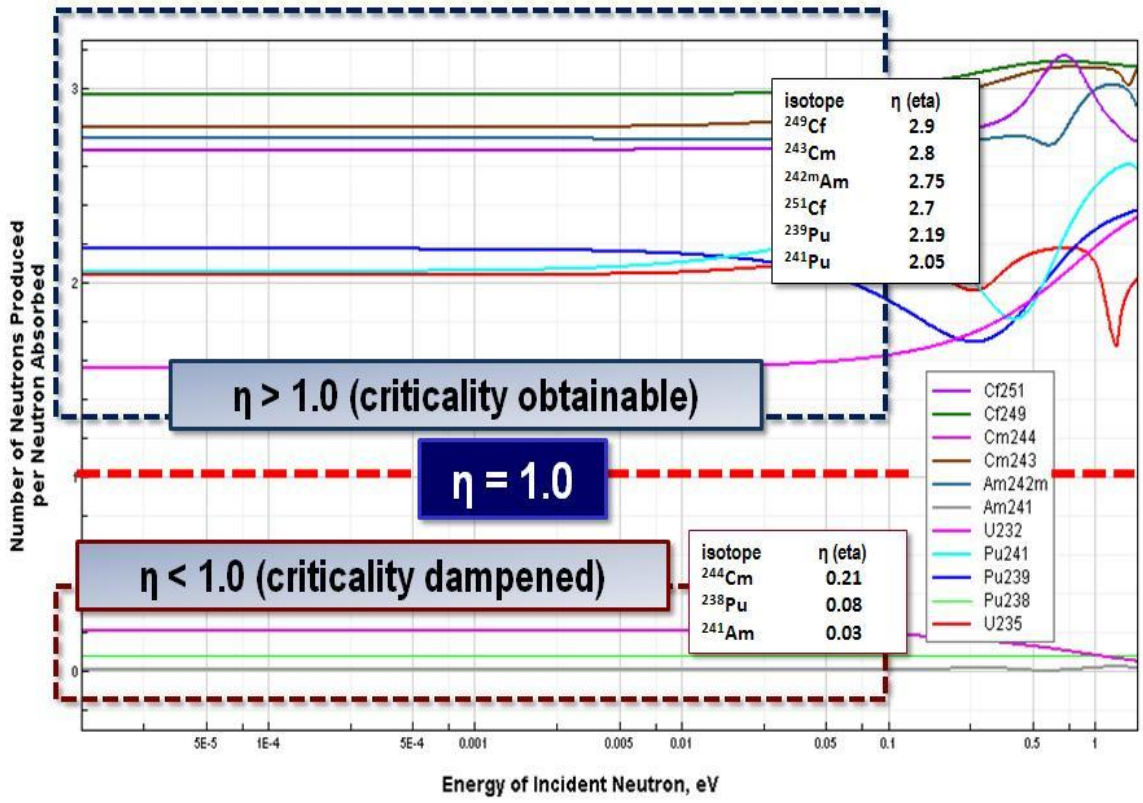

Figure 6. Neutrons Produced per Neutron Absorbed in the Thermal Spectrum

The ability to sustain a fission chain reaction with a given fuel element is hindered for actinide isotopes having η less than unity. Therefore, in this thesis, ^{241}Am, ^{238}Pu and ^{244}Cm will be discarded as potential candidates for energy sources. Additionally, ^{232}U shows marginal ability for chain reaction sustainment and will also be eliminated from further consideration in this thesis. It is recognized that for this thesis, the results apply to pure isotopes only.

The effective multiplication factor, K_{eff} (obtained computationally in section III.B.) is a measure of criticality accounting for neutron leakage. Specific power, P_i is the amount of energy produced per unit time per unit mass for pure fuel elements. K_{eff} and P_i are plotted in Figure 7. The data shows that criticality is obtainable using ^{242m}Am, ^{249}Cf and ^{251}Cf. ^{243}Cm has the highest P_i per pure isotopic concentration, while the isotope with the lowest P_i is ^{242m}Am.

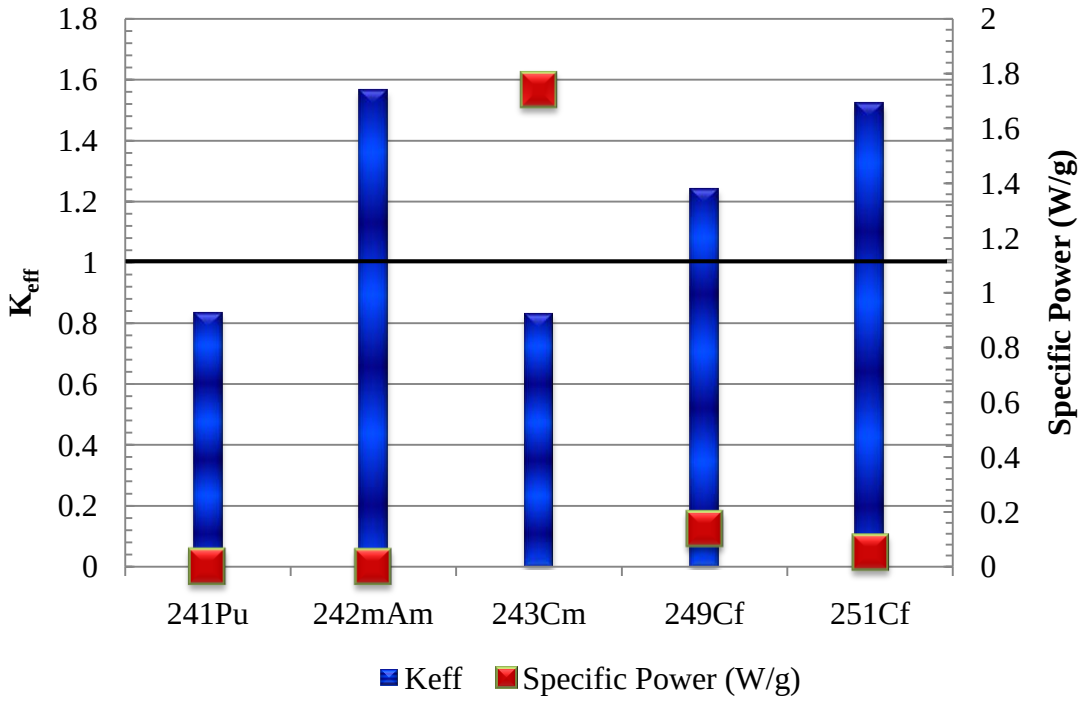

Figure 7. Pure Isotope Specific Power (W/g)

Low decay heat may be advantageous for certain space power applications in order to avoid extreme static heat management requirements.

II.B. Fission Fragments as Energy Carriers

In nuclear fission reactions, prompt neutrons and gamma rays are emitted along with the emission of FF particles as shown in equation (2), where X_1 and X_2 are fission fragments, Z is the atomic number and A is the mass number. FF particles are radioactive and remain on the order of minutes before decaying. These fragment particles tend to fall into two groups, a lighter group (mass number between 80-110) and a heavier group (mass number between 120-155).

$$ {}^{1}_{0}n + {}^{A}_{Z}X \rightarrow ({}^{A+1}_{Z}X)^{*} \rightarrow {}^{A_1}_{Z_1}X_1 + {}^{A_2}_{Z_2}X_2 + \nu_{fp} * {}^{1}_{0}n + \sim 200\, MeV \qquad (2) $$

In equation (2), ν_{fp} is defined as the number of prompt neutrons produced per fission. JANIS was utilized to examine FF particle mass distributions. Independent fission yields of particular nuclides can be determined directly from neutron-induced fission prior to beta decay or delayed neutron interactions. Conversely, cumulative fission yield takes into account all decay branches after fission plus delayed neutron interactions [27]. In this thesis, only independent mass yields are presented. Independent fission yield data is shown in Figures 8-11.

JEFF 3.1 (Joint Evaluated Fission and Fusion) data is used in this work to construct some of the mass data plots. The JEFF 3.1 nuclear data library, released in 2005, has a complete suite of nuclear data and contains general purpose nuclear data evaluations compiled at the NEA Data Bank with other laboratories. The JEFF 3.1 data

set contains radioactive decay data, activation data and fission yields data. The JEFF 3.1 library contains neutron reaction data, incident proton data and thermal neutron scattering law data in the ENDF6 format, which is used in this thesis. Figure 8 shows mass distribution data for neutron fission under fast, slow and thermal neutron incident energies.

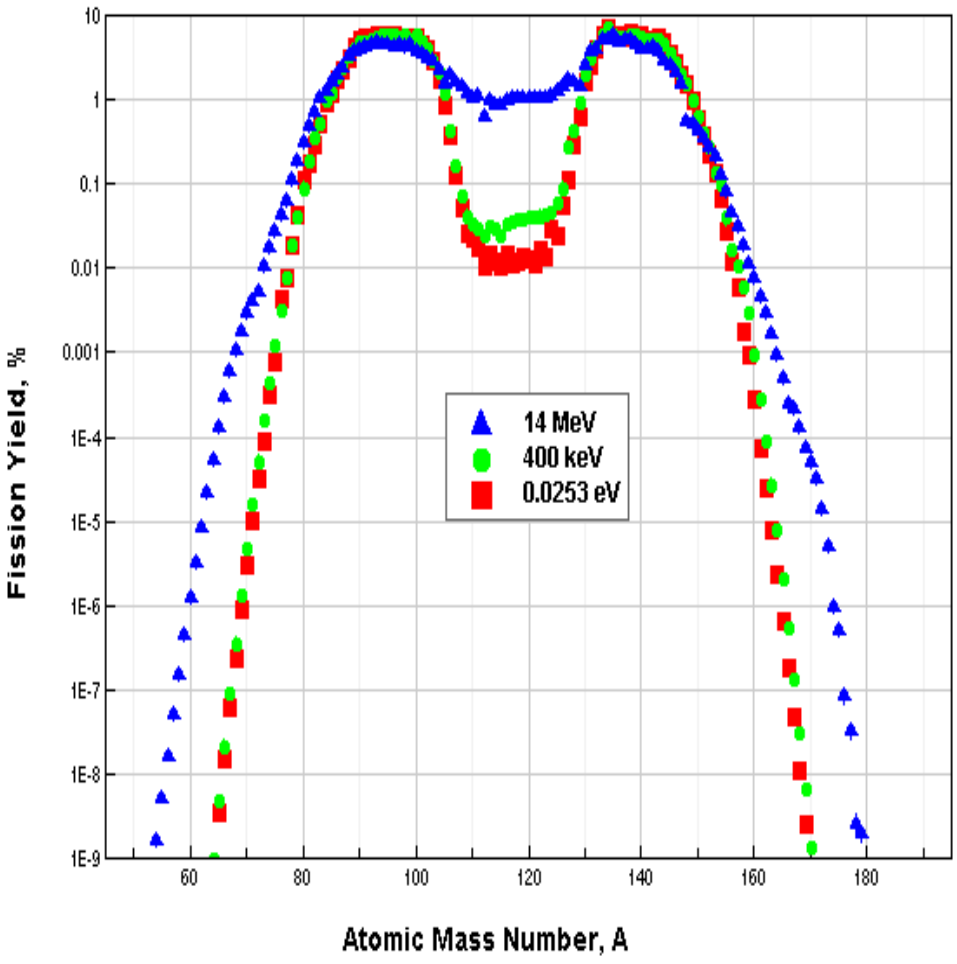

Figure 8. Independent Fission Yields for ^{235}U

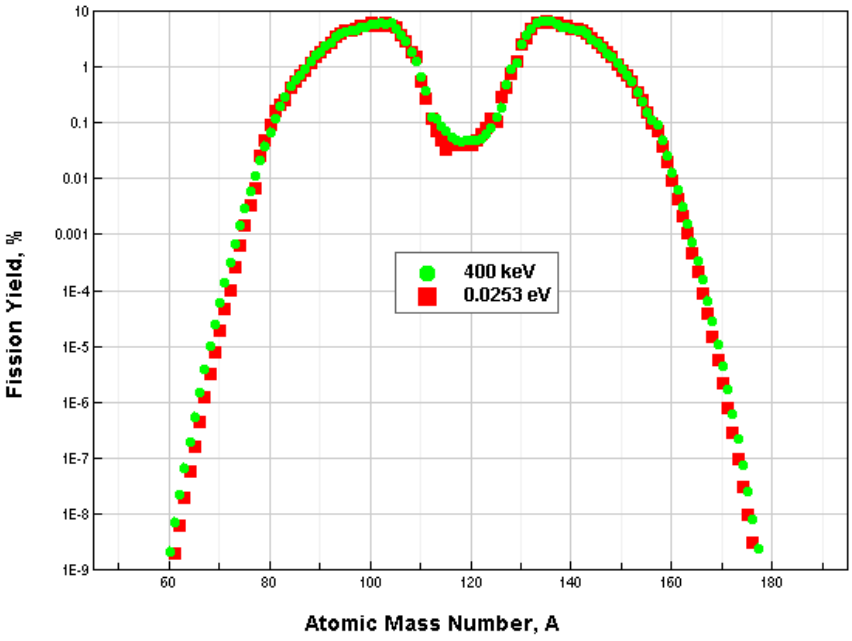

(a)

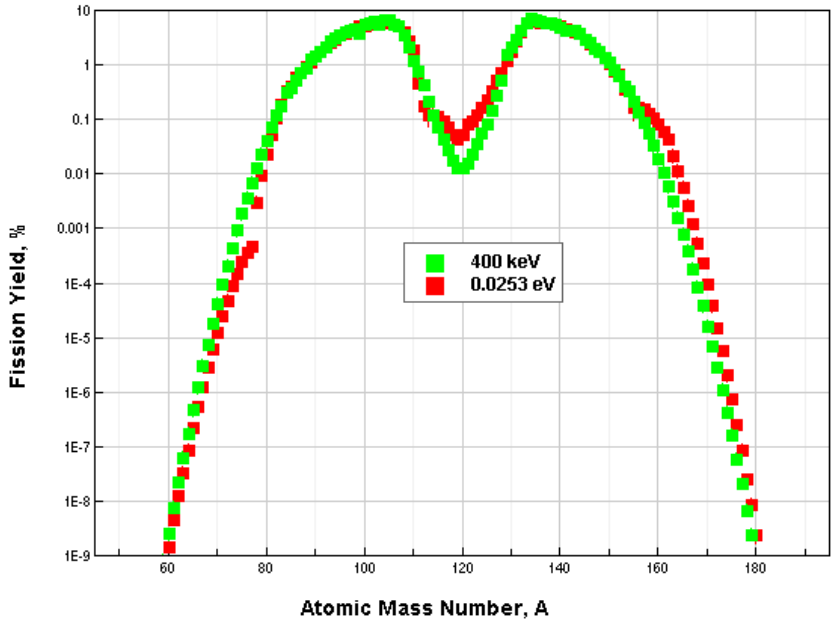

(b)

Figure 9. Independent Fission Yields for a) ^{239}Pu and b) ^{241}Pu

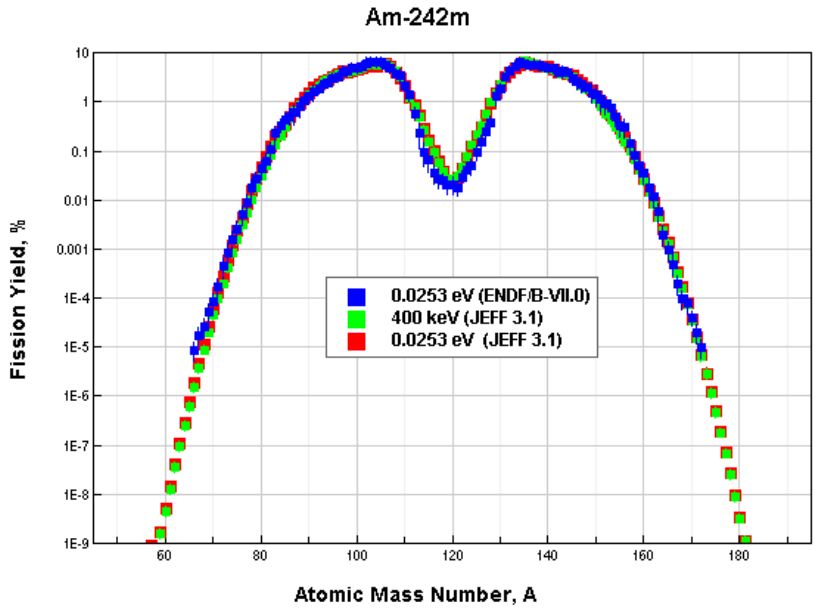

(a)

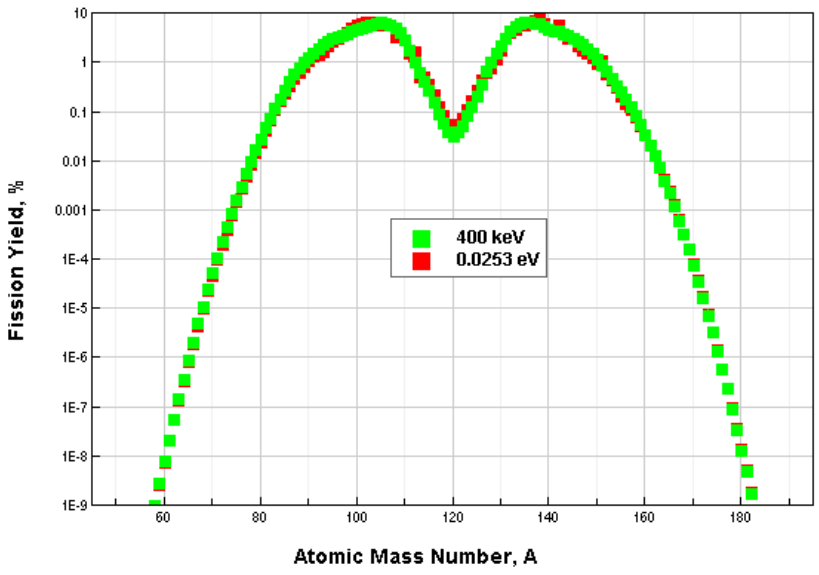

(b)

Figure 10. Independent Fission Yields for a) ^{242m}Am and b) ^{243}Cm

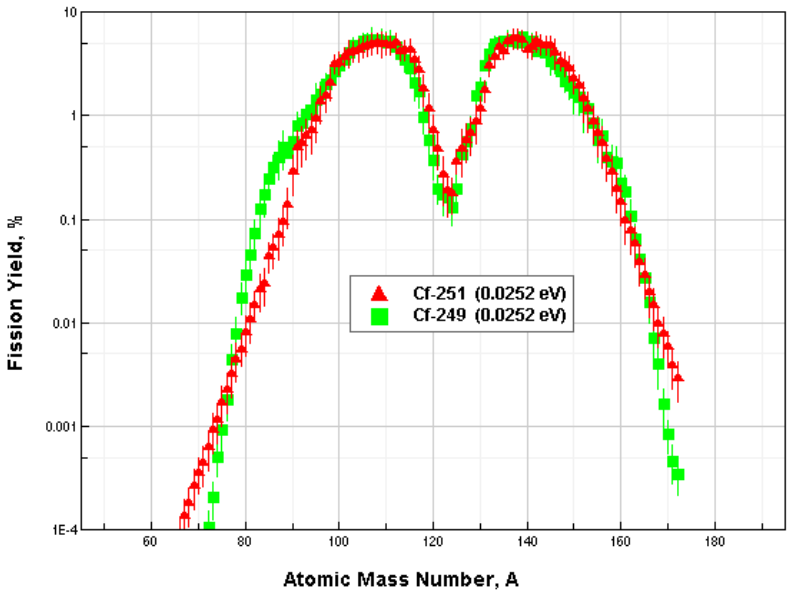

Figure 11. Independent Fission Yields for ^{249}Cf and ^{251}Cf

Analysis of fission yield data provides light and heavy ion fragment masses, as shown in Table 5.

Table 5. Light and Heavy Fission Fragment Masses

	Peak Value of Light FF Mass (amu)	**Peak Value of Heavy FF Mass (amu)**
^{235}U	95	138
^{239}Pu	103	134
^{241}Pu	104	134
^{242m}Am	106	135
^{243}Cm	103	134
^{249}Cf	108	139
^{251}Cf	112	137

The kinetic energy of particles emitted during fission are shown in Tables 6-8. Immediate, delayed and total energy states are provided. Analysis of energy distributions from neutron fission indicate that ^{242m}Am and ^{243}Cm provide higher FF kinetic energies (approximately 10-15 MeV higher) relative to baseline uranium and plutonium fuels. Prompt neutron, delayed γ-ray, β-particle and neutrino kinetic energies appear similar for all actinides isotopes as a result of thermal neutron-induced fission.

Table 6. Components of Immediate Fission Energy Release for ^{235}U, ^{239}Pu, ^{241}Pu, ^{242m}Am, ^{243}Cm

Isotope	**Prompt Kinetic Energy Release (MeV)**		
	Fission Fragments	**Prompt Neutrons**	**Prompt γ-rays**
^{235}U	169.0 ± 0.5	4.70 ± 0.07	6.2 ± 0.5
^{239}Pu	175.2 ± 0.1	5.3 ± 0.1	7.10 ± 0.2
^{241}Pu	175.7 ± 0.3	5.0 ± 0.2	7.0 ± 0.4
^{242m}Am	182.0 ± 0.2	4.8 ± 0.3	1.0 ± 0.4
^{243}Cm	186.0 ± 0.6	6.0 ± 0.4	6.0 ± 0.2

Table 7. Components of Delayed Fission Energy Release for ^{235}U, ^{239}Pu, ^{241}Pu, ^{242m}Am, ^{243}Cm

Isotope	Delayed Kinetic Energy Release (MeV)			
	Delayed Neutrons	**Delayed γ-rays**	**Total Energy of β-particles**	**Energy of Neutrinos**
^{235}U	0.010 ± 0.001	6.30 ± 0.05	6.51 ± 0.05	8.73 ± 0.07
^{239}Pu	0.0026 ± 0.0004	5.12 ± 0.06	5.34 ± 0.06	7.11 ± 0.09
^{241}Pu	0.0052 ± 0.0003	6.42 ± 0.04	6.50 ± 0.05	8.89 ± 0.03
^{242m}Am	0.0013 ± 0.0005	7.0 ± 0.6	7.51 ± 0.06	10.0 ± 0.6
^{243}Cm	0.011 ± 0.004	6.11 ± 0.05	6.32 ± 0.04	8.42 ± 0.06

In the FFMC reactor concept, ejected particles must be manipulated by electromagnetic fields. FF particles are highly charged and the ability to stop and direct them is a function of particle energy and charge.

Table 8. Total and Recoverable Fission Energy Release for ^{235}U, ^{239}Pu, ^{241}Pu, ^{242m}Am, ^{243}Cm

Isotope	Total Energy Release (MeV)	Recoverable Energy Release (MeV)	Recoverable Energy Fraction Released with FF (%)
^{235}U	202.0 ± 0.1	193.2 ± 0.2	0.956 ± 0.004
^{239}Pu	207.3 ± 0.2	200.8 ± 0.2	0.968 ± 0.001
^{241}Pu	210.8 ± 0.6	201.2 ± 0.5	0.950 ± 0.002
^{242m}Am	212.0 ± 1	202.6 ± 0.1	0.955 ± 0.002
^{243}Cm	220.1 ± 0.4	212.2 ± 0.3	0.961 ± 0.003

Beginning with FF kinetic energy, particle masses and energy per FF, the charge associated with each FF, q can be determined according to equation (3) where Z is the atomic number, v is the fragment velocity, $k = 0.6$, $v_o = 3.6 \times 10^8$ cm/s and $\alpha = 0.45$ [28].

$$q = Z\left(1 + \left(\frac{v_0 Z^{\alpha}}{v}\right)^{1/k}\right)^{-k} \tag{3}$$

The particle kinetic energy, E, can be used to compute the energy per charge (E/q) ratio which provides a measure of the required voltage to stop FF particles. The charge and E/q ratio are presented in Table 9.

Table 9. FF Energy, Charge and E/q Ratio

Actinide Isotope		**Energy, E (MeV)**	**Charge, q (e)**	**E / q (MV)**
^{235}U	Light FF	100.1	23.33	4.29
	Heavy FF	68.9	21.72	3.17
^{239}Pu	Light FF	99.4	23.82	4.17
	Heavy FF	76.4	22.59	3.38
^{241}Pu	Light FF	98.7	23.69	4.17
	Heavy FF	76.6	22.59	3.39
^{242m}Am	Light FF	102.9	24.10	4.27
	Heavy FF	79.1	22.87	3.46
^{243}Cm	Light FF	105.1	24.25	4.34
	Heavy FF	80.8	23.08	3.50

The data indicates that FF particles are highly charged particles having charges of +20e (where e is the electric charge carried by a single proton) or higher. Figure 12 shows that for heavier fission fragments, the E/q ratio ranges from 3.17-3.5 MV, while light FF particles have E/q ratios from 4.17-4.34 MV. Larger voltages are required for lighter FF particles to be stopped in an electromagnetic field, while less voltage may be

applicable to slow lower mass FF particles. In either case, given the selected isotope fission fragment ions, a 5 MV potential should allow adequate stopping power for FF's.

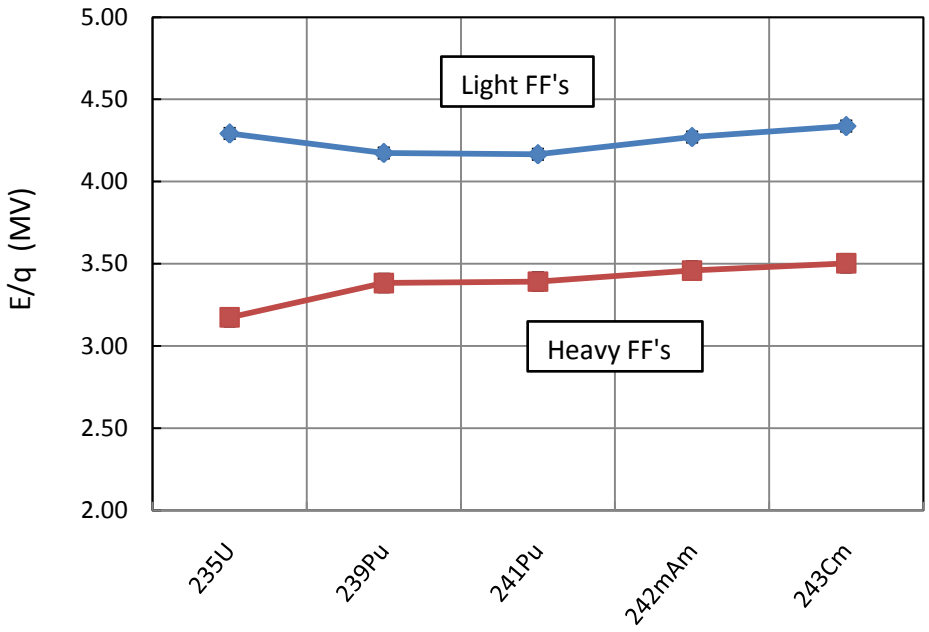

Figure 12. E/q Resulting from Thermal Neutron Induced Fission of ^{235}U, ^{239}Pu, ^{241}Pu, ^{242m}Am, ^{243}Cm

Light and heavy fission fragment particle velocities were computed and shown in Table 10. The range of projectile particles ranges from 0.032c to 0.047c.

Table 10. Computed FF Velocities

Isotope	Light FF Velocity		Heavy FF Velocity	
	m/s	% c	m/s	% c
^{235}**U**	1.43×10^{7}	0.047 c	9.82×10^{6}	0.032 c
^{239}**Pu**	1.36×10^{7}	0.045 c	1.05×10^{7}	0.035 c
^{241}**Pu**	1.35×10^{7}	0.045 c	1.05×10^{7}	0.035 c
^{242m}**Am**	1.37×10^{7}	0.045 c	1.06×10^{7}	0.035 c
^{243}**Cm**	1.40×10^{7}	0.046 c	1.08×10^{7}	0.036 c

* c is the speed of light

SRIM (Stopping and Range of Ions in Matter) [29], a 3D Monte Carlo computational code for computing energy loss of ions in solids, liquids and gases, was utilized to examine fission fragment particle escape through thin layers of ^{242m}Am. A 100 MeV rhodium ion was injected into a 3 micron layer of ^{242m}Am. The result indicates, according to Figure 13(a) that fuel layers greater than 3 microns thick prevent particles from escaping. The same 100 MeV rhodium ion was then projected into a 1 micron thick layer of ^{242m}Am. According to Figure 13(b) a 1 micron layer of ^{242m}Am will allow a significant fraction of FF particles to escape the layer. The results indicate that more than 90% of the fission fragments will exit the 1 micron thick fuel layer. This finding is in agreement with more detailed analysis in related publications [24]. In the present analysis, a 1-2 micron layer of fuel appears to satisfy the requirement to allow FF particles to escape the fuel layer. All other near peak-mass fragment ions exhibit similar behavior and appear to escape the micron thick fuel layer for energies greater than 80 MeV.

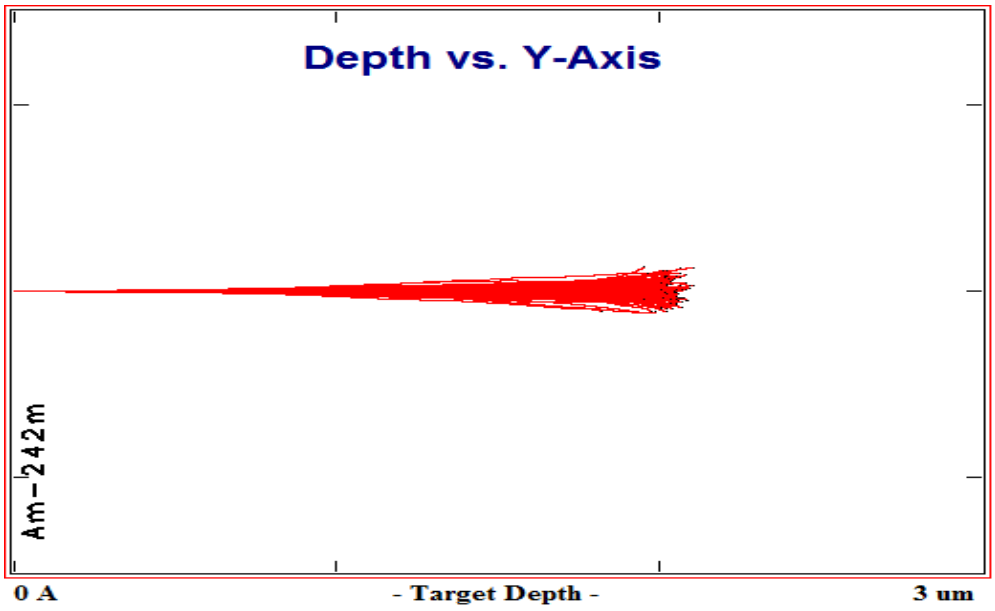

(a)

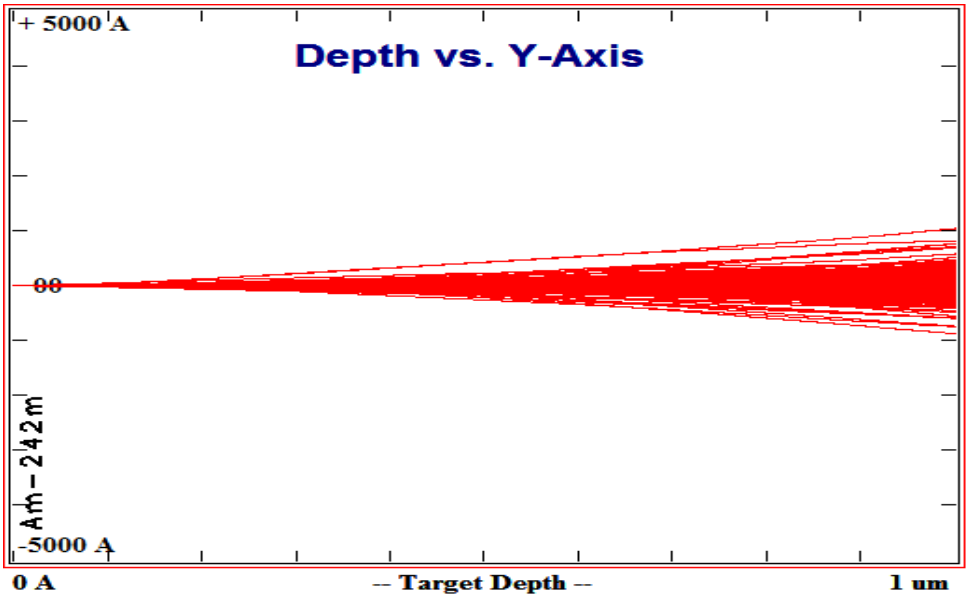

(b)

Figure 13. 100 MeV Rhodium Ion into a) 3 μm and b) 1 μm layer of ^{242m}Am

II.C. Potential Actinide Candidates for Deep Space Applications

The requirements for deep space power or propulsion drive the search for acceptable actinide-based energy sources. For long term operation, successful actinide candidates must have half-life properties that support beginning-of-mission (BOM) to end-of-mission (EOM) power requirements. For deep space or interstellar operation, this generally translates to life-time properties greater than 20 years. In this survey of higher actinides ^{241}Pu and ^{244}Cm are excluded from further consideration based on half-lives of 14.35 and 18.1 years, respectively. In addition, for pre-launch operations, ^{241}Pu and ^{244}Cm post significant radiological hazards compared to other isotopes. The specific activity of ^{241}Pu is 100 Ci/g and that of ^{244}Cm is approximately 82 Ci/g. The next highest specific activity is ^{243}Cm at 52 Ci/g. Although excluded for half-life and high specific activity, it is notable that ^{244}Cm has the lowest thermal fission cross section of the surveyed actinides, also making it undesirable for deep space applications.

The highest thermal fission cross section of the surveyed isotopes is ^{242m}Am, followed by ^{251}Cf and ^{249}Cf. As noted previously, ^{242m}Am has a significantly higher (see Figure 4) thermal fission cross section than baseline isotopes ^{238}Pu, ^{239}Pu, ^{241}Pu or ^{235}U. The very high thermal fission cross section property of ^{242m}Am is attractive for energy production. Actinides ^{251}Cf and ^{249}Cf also have attractive fission cross section properties.

The requirement for the reactor core to feasibly sustain a chain reaction is dependent upon a fuel's ability to produce extra neutrons from fission. The number of

neutrons produced per neutron absorbed for ^{242m}Am is found to be superior to any other actinide. Conversely, as shown in Figure 6, η is less than unity for ^{241}Am, ^{238}Pu and ^{244}Cm. These isotopes cannot maintain criticality and are not adequate for satisfying deep space power or energy source requirements. Uranium-232 is also found to have only marginal values for η and is therefore not suited as an innovative energy source.

High FF kinetic energies are desired for thrust and energy production. Particles captured by magnetic field lines should be highly energetic and have significant recoverable energy. Compared to baseline isotopes, ^{242m}Am and ^{243}Cm have the highest FF kinetic energy and recoverable energy release from thermal neutron induced nuclear fission.

Charges in motion, the most fundamental definition of current, can be obtained using high ionic charges. Data from Table 9 indicates that higher charges are possible with ^{242m}Am and ^{243}Cm, slightly higher than what may be obtain from the baseline uranium and plutonium actinides.

Curium is not found naturally and is produced from nuclear reactors through neutron capture reactions from plutonium or americium. The isotope ^{243}Cm has a relatively low half-life of 29 years and a medium grade specific activity of 52 Ci/g. In addition, ^{243}Cm produces significant amounts of prompt γ-ray radiation. For example, 6.92 MeV prompt γ-rays are emitted from ^{243}Cm, while 1.2 MeV prompt γ-rays are emitted from ^{242m}Am. In addition, higher energy prompt neutrons are emitted from ^{243}Cm.; thus, ^{243}Cm will not be implemented as a majority fuel element in designing the reactor core.

II.D. Sustainability of Actinide-Based Nuclear Fuel Systems

The ^{242m}Am isomer exhibits one of the highest known thermal neutron fission cross sections. The thermal neutron cross section of ^{242m}Am is approximately 6000 barns. The ^{242m}Am thermal capture cross section is low relative to other actinides. In addition, the number of neutrons produced per fission is high compared to uranium, plutonium and other actinides. These properties, coupled with a half-life of 141 years, provide strong support for investigating novel uses of this isotope, including advanced deep space power and energy sources. The major disadvantage of ^{242m}Am is its availability.

According to [29], the world-wide production rate of ^{242m}Am is approximately 2.74 kg (6.04 lbs) per year. One reaction which creates ^{242m}Am arises from the plutonium decay from spent nuclear fuel in light water reactors (LWR). Specifically, ^{242m}Am can be produced from ^{241}Pu as shown from the radioactive decay diagram in Figure 14.

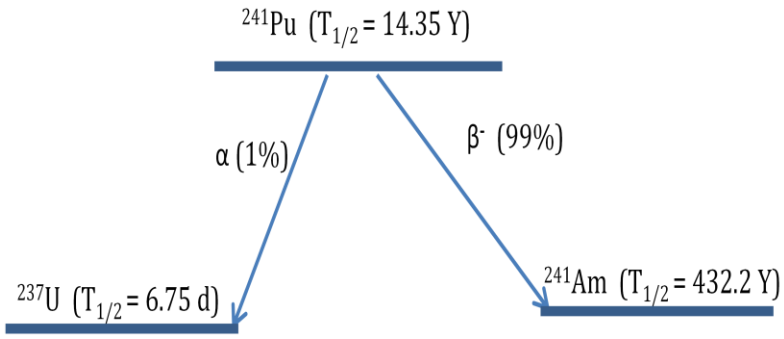

Figure 14. Decay of ^{241}Pu into ^{241}Am

After ^{241}Am is created from decay of ^{241}Pu, the isomer ^{242m}Am can be produced from the neutron or radiative capture reaction ^{241}Am(n,γ)^{242m}Am. Equation (4) shows the production of ^{242m}Am via neutron capture of ^{241}Am.

$$^{241}\text{Am} + {}^{1}_{0}n \longrightarrow {}^{242m}\text{Am} + \gamma \qquad (4)$$

Several methods to produce ^{242m}Am have been proposed in previous literature including particle accelerators and nuclear reactors [24]. In order to maintain a viable deep space power program based on ^{242m}Am fuel, a production and manufacturing system must be executed. The selection of higher actinides for implementation as a FFMCR fuel concept have been down-selected to three isotopes (^{242m}Am, ^{249}Cf and ^{251}Cf). In this thesis, these isotopes are applied in reactor core modeling and analysis in Chapter III.

CHAPTER III

REACTOR PERFORMANCE

Nuclear criticality and fuel depletion analysis will be performed using SCALE6.0 (Standardized Computer Analysis for Licensing Evaluation), a modular computational code system [30]. In particular, SCALE provides the following analysis capabilities:

- Problem Dependent Cross Section Processing;
- Flexible Mesh Discrete Ordinate Reactor and Lattice Physics Analysis;
- Monte Carlo Criticality Safety Analysis;
- Sensitivity and Uncertainty Analysis;
- 3-D Monte Carlo Depletion and Spent Fuel Analysis;
- Advanced 3-D Visualization.

SCALE consists of modules of code which are partitioned in sections called functional and control modules. Control modules perform sequences, prepare inputs, conduct data transfer and other execution level tasks. Functional modules contain fundamental physics properties and processes. In this thesis, the Transport Rigor Implemented with Time-dependent Operation for Neutronic depletion (TRITON) SCALE control module will be the central module for performing reactor core characterization and depletion physics calculations. There are five computational sequences within TRITON: T-XSEC, T-NEWT, T-DEPL, T5-DEPL and T6-DEPL. For purposes of this thesis, the T5-DEPL analytical depletion sequence using KENO V.a (a

3D Monte Carlo code for computing neutron multiplication factors) is used, as shown in Figure 15.

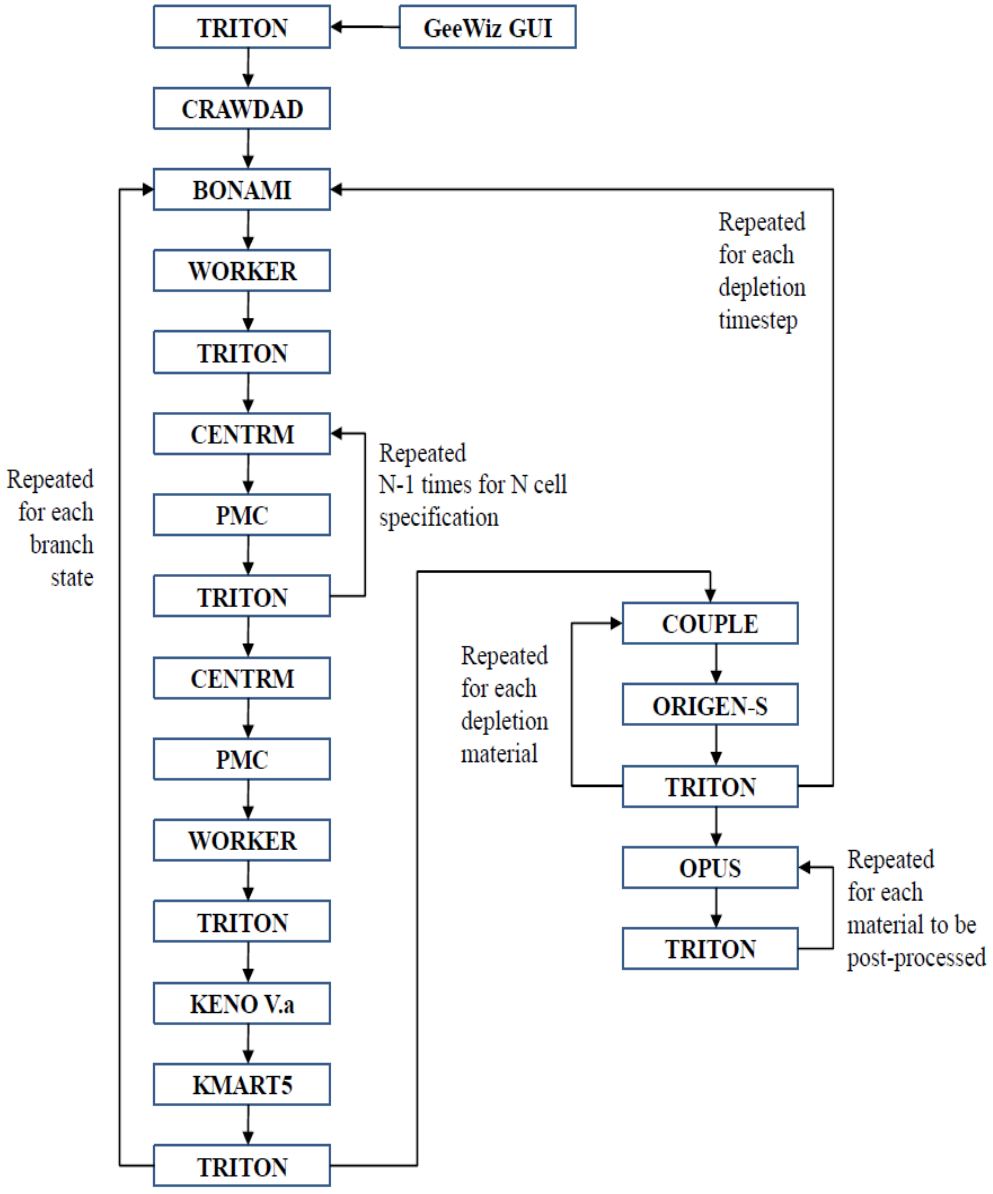

Figure 15. TRITON T5-DEPL Depletion Sequence Using KENO V.a

The graphical user interface (GUI) Graphically Enhanced Editing Wizard (GeeWiz) within SCALE assists with creating, entering and executing SCALE input files in Windows format [31]. GeeWiz accepts input such as cell structures, mixtures, reaction types, geometry and other initialization parameters.

The CRAWDAD (Code to Read And Write Data for Discretized solution) utility module reads nuclear data from SCALE-6 general point-wise library files and writes it in a format needed for the discretized energy solution used in the CENTRM module. The CRAWDAD section of code is generally run automatically [31].

Cross section processing is accomplished using the Bondarenko AMPX Interpolator (BONAMI). BONAMI performs Bondarenko calculations for resonance self-shielding in the unresolved resonance energy range. Essentially, the Bondarenko method computes effective cross sections. The effective cross section can be written as the ratio shown in equation (5). The goal is to determine the flux, $\phi(u)$, assuming the cross section $\sigma(u)$ can be determined [32]. In equation (5), $\sigma(u)$ is the cross section as a function of lethargy, $\phi(u)$ is the flux per unit lethargy and g is the group number.

$$\overline{\sigma_g} = \frac{\int_g du\,\sigma(u)\phi(u)}{\int_g du\,\phi(u)} \tag{5}$$

The fundamental equation behind the Bondarenko method is shown in equation (6), where $\sum_t$ is the total macroscopic cross section.

$$\phi(u) \sim \frac{1}{\Sigma_t(u)} \tag{6}$$

Equation (6) relates the flux per unit lethargy and the macroscopic total cross-section. The microscopic cross sections can then be evaluated.

The sub-module WORKER is used to read cross-section libraries [33]. The WORKER module is applied in all SCALE system analytical sequences that use CENTRM and PMC (discussed below) to perform problem-dependent cross-section processing. This section of code converts data from the AMPX master library into an AMPX working library format to be used by other modules [34].

TRITON uses the Continuous Energy Transport Module (CENTRM) to perform resolved resonance evaluations [35]. The CENTRM module is designed to compute continuous neutron energy spectra by solving the Boltzmann equation, with the goal of determining specific fluxes on fine energy mesh structures for full or continuous spectrum across most reactor physics energy ranges [35].

Multigroup data processing is accomplished by using the Produce Multigroup Cross (PMC) module, which accepts input from the CENTRM module. The PMC code is used to produce problem-dependent, self-shielded multi-group data, by means of a weighting function which represents the fine-structure variation in the neutron energy spectrum for a one-dimensional model [35].

The T5-DEPL sequence applies the KENO V.a module, a three-dimensional (3-D) Monte Carlo criticality transport program to determine fluxes [36]. The TRITON modules and associated functions used to calculate reactor core theoretical performance in this thesis are provided in Table 11.

Table 11. SCALE and TRITON Computational Modules and Functions

Module	Function
CRAWDAD	Reads nuclear data from SCALE6 general point-wise library files and writes it in a format needed for the discretized energy solution used in the CENTRM module
BONAMI	Performs Bondarenko calculations for resonance self-shielding in the unresolved resonance energy range
WORKER	Utility used to read cross-section libraries
CENTRM	Continuous energy flux spectra for multi-group cross-section processing
PMC	Accepts input from the CENTRM module; used to produce problem-dependent, self-shielded multi-group data
KENA V.a	3-D Monte Carlo code for calculation of neutron multiplication factors
COUPLE	Interface module for preparing cross-section and spectral data for the ORIGEN-S module
ORIGEN-S	Point depletion and decay code to calculate isotropic, decays radiation source terms and curie levels
OPUS	Produces an output file and plot data from ORIGEN-S output code; computes reactor fuel depletion, activation and fission- product buildup, and the associated photon and neutron source spectra.

III.A. Energy System Design

The most critical component in examining the viability of the FFMCR concept design is the fuel element. The fuel element is a graphite fiber with a nano layer of fuel. The distance between fuel elements is 0.017 cm. The fuel layers are stacked on a fuel sub-assembly frame in a cylindrical assembly configuration. Neutron multiplicity is enhanced by using multiple layers of reflector material. The FFMCR design parameters assumed for this work are shown in Tables 12-13. The vacuum vessel, reflector layers and fuel assembly are shown in Figure 16 and the final whole-core 3-D reactor design in shown in Figure 17. One unique feature of the FFMCR design is that both ends of the reactor core act as particle collectors, creating multiple points for propulsive force or power generation.

Table 12. FFMCR Core Design Components

Nuclear Reactor Core:	
Outer Core Radius	414.5 cm
Outer Core Length	740.0 cm
Total Number of Fuel Assemblies	83
Total Number of Sub-Assemblies	139440
Total Number of Fuel Elements	1.39×10^{10}
Total Fuel Loading	24 kg (approximately)
Fuel Assembly Design:	
Geometry	Cylindrical
Outer Fuel Assembly Length	140.0 cm
Outer Fuel Assembly Radius	60.0 cm
Fuel Sub-Assembly Design:	
Geometry	Rectangular Frame - Fuel Coated Fibers
Outer Fuel Sub-Assembly Length	20.0 cm
Outer Sub-Assembly Width	5.0 cm
Outer Sub-Assembly Depth	1.0 cm
Number of Fuel Elements per Sub Assembly	1×10^{5}
Fuel Element Design:	
Type	Fuel Coated Graphite Layer
Fuel Layer	
Fuel	100% (^{242m}Am)
Thickness	0.0001 cm
Graphite Fiber	
Radius	0.00015 cm
Active Length	1.0 cm
Burnable Absorber Doping	20.0 %
Fuel Loading per Element	1.722×10^{6} g

Mutliple reflector regions have been added to provide room for expansion and potentially superconducting magnetic installation. The reflector region may be changed pending desired power level outputs and neutron confinement.

Table 13. FFMCR Reflector and Cavity Design Parameters

Nuclear Reactor Reflector:	
Material	Nuclear grade graphite
Central Cylindrical Section	
- Peripheral hemispherical A	250.5 cm
- Peripheral hemispherical B	100.0 cm
- Inner Radius	100.0 cm
- Outer Radius	690.0 cm
Nuclear Reactor Cavity:	
Radius	535.0 cm
Length	1810.0 cm
Volume Fractions:	
Sub-Assembly (FE/SA)	1.9635E-4
Assembly (FE/FA)	2.083E-5
In Reactor Core (FE/NRC)	6.854E-6
Distance between fuel elements:	0.017 cm

.

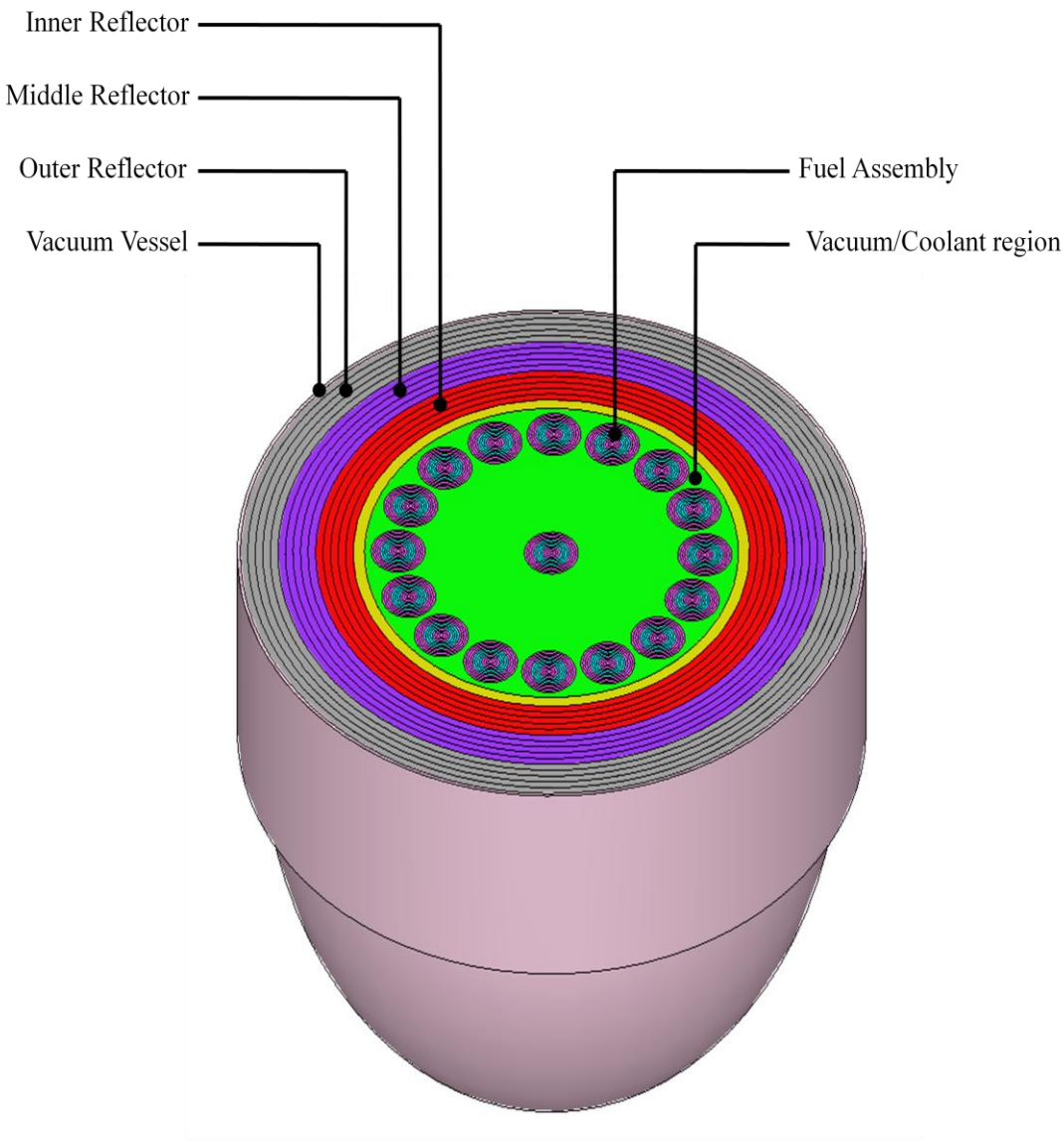

Figure 16. Main Components of the Reactor Core Design

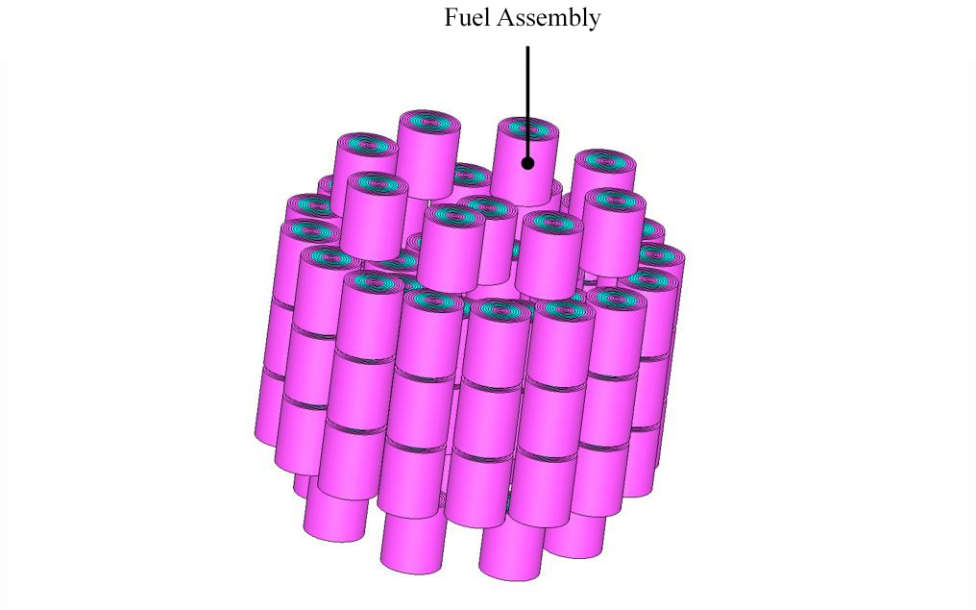

(a)

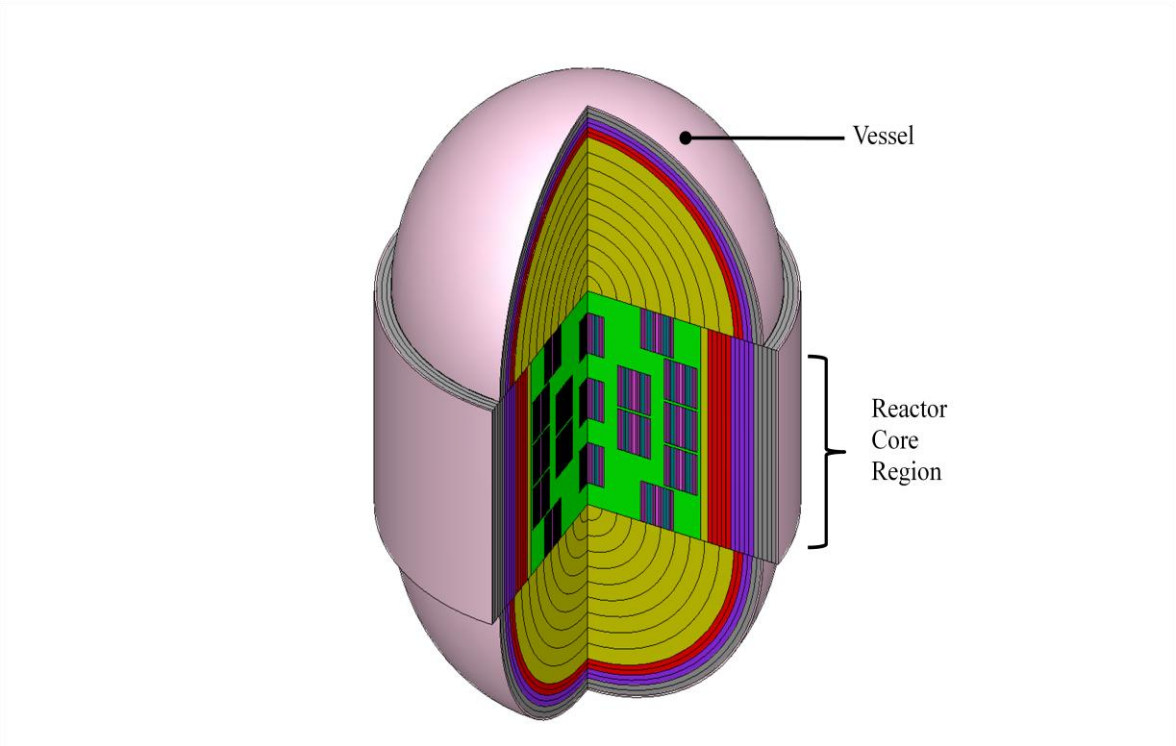

(b)

Figure 17. a) Fuel Assembly Units and b) 3-D FFMCR Model

III.B. Performance Analysis

Three-dimensional Monte Carlo analysis of baseline and higher actinides shows that the highest K_{eff} for the FFMCR configuration is obtained using ^{242m}Am, with a computed value of 1.5649. System criticality is obtainable for ^{242m}Am, ^{249}Cf and ^{251}Cf. Calculated K_{eff} for pure isotopic fuels is shown in Table 14. Baseline isotopes (^{235}U, ^{239}Pu, ^{241}Pu) proposed for conventional nuclear reactor designs, as well as ^{243}Cm, are found to be unable to sustain criticality as pure isotopic fuels in the FFMCR concept. The average number of neutrons produced per fission event, $\bar{\nu}$, is found to be highest when utilizing the ^{251}Cf isotope.

Table 14. Criticality Parameters for Pure Isotopic Concentrations at 900K

Fuel	K_{eff}	$\bar{\nu}$	**λ, cm**
T = 900 K			
^{235}U	0.4681 ± 0.0008	2.43691 ± 0.00001	9.784 ± 0.009
^{239}Pu	0.6995 ± 0.0009	2.88932 ± 0.00001	9.510 ± 0.009
^{241}Pu	0.835 ± 0.001	2.95324 ± 0.00001	9.50 ± 0.01
^{242m}Am	1.560 ± 0.002	3.26432 ± 0.00001	8.96 ± 0.01
^{243}Cm	0.833 ± 0.001	3.43069 ± 0.00002	9.723 ± 0.009
^{249}Cf	1.248 ± 0.007	4.06058 ± 0.00002	9.46 ± 0.01
^{251}Cf	1.519 ± 0.001	4.14045 ± 0.00001	8.97 ± 0.01

The mean free path, λ, for neutrons in all actinides surveyed in this work is approximately 9 cm as shown in Table 14 .The average energy of incident neutrons causing fission is found to be approximately 0.05-0.08 eV. Neutron generation time, $\overline{\Lambda}$, is found to be shortest when utilizing ^{242m}Am and ^{251}Cf. The neutron lifetime and generation times are shown in Table 15. Group fission data is shown in Table 16.

Table 15. Neutron Lethargy, Lifetime and Generation Time for Pure Isotopic Concentrations

Fuel	**Energy of average lethargy of fission (eV)**	**Neutron Lifetime (s)**	**Neutron Generation Time, $\overline{\Lambda}$ (s)**
T = 900 K			
^{235}U	0.0506 ± 0.0001	0.0232 ± 0.0003	0.02743 ± 0.00005
^{239}Pu	0.0723 ± 0.0001	0.0184 ± 0.0002	0.02049 ± 0.00003
^{241}Pu	0.0719 ± 0.0001	0.0176 ± 0.0002	0.01934 ± 0.00003
^{242m}Am	0.0833 ± 0.0001	0.0098 ± 0.0002	0.00842 ± 0.00001
^{243}Cm	0.0676 ± 0.0002	0.0213 ± 0.0003	0.02486 ± 0.00005
^{249}Cf	0.0587 ± 0.0001	0.0163 ± 0.0002	0.01807 ± 0.00003
^{251}Cf	0.0742 ± 0.0001	0.0098 ± 0.0001	0.00972 ± 0.00001

Fuel lifetime can potentially be extended if burnable neutron absorbing additives are utilized to reduce beginning of life (BOL) excess reactivity of the fuel. In this case, a subsequent slow discharge during operation to compensate fuel depletion effects can be obtained.

Table 16. Group Fission Data at 900 K for Pure Isotopic Concentrations

Fuel	**Average Energy Group Fission Occurs (eV)**
T = 900 K	
^{235}U	37.434 ± 0.006
^{239}Pu	36.253 ± 0.006
^{241}Pu	36.373 ± 0.006
^{242m}Am	35.834 ± 0.006
^{243}Cm	36.47 ± 0.01
^{249}Cf	36.984 ± 0.006
^{251}Cf	36.045 ± 0.006

It is noted that previous work has shown that a more complex analysis should be carried out to incorporate burnable absorbers into nano layer fuel elements [24]. The cross-sections for ^{135}Xe, ^{167}Er, ^{177}Hf, ^{157}Gd and ^{10}B burnable neutron absorbers are shown in Figure 18.

Preliminary calculations utilizing 80% pure isotopic concentrations with 20% burnable absorber infused into the fuel verify that K_{eff} is reduced the most when utilizing ^{135}Xe and least when incorporating ^{177}Hf (see Table 17).

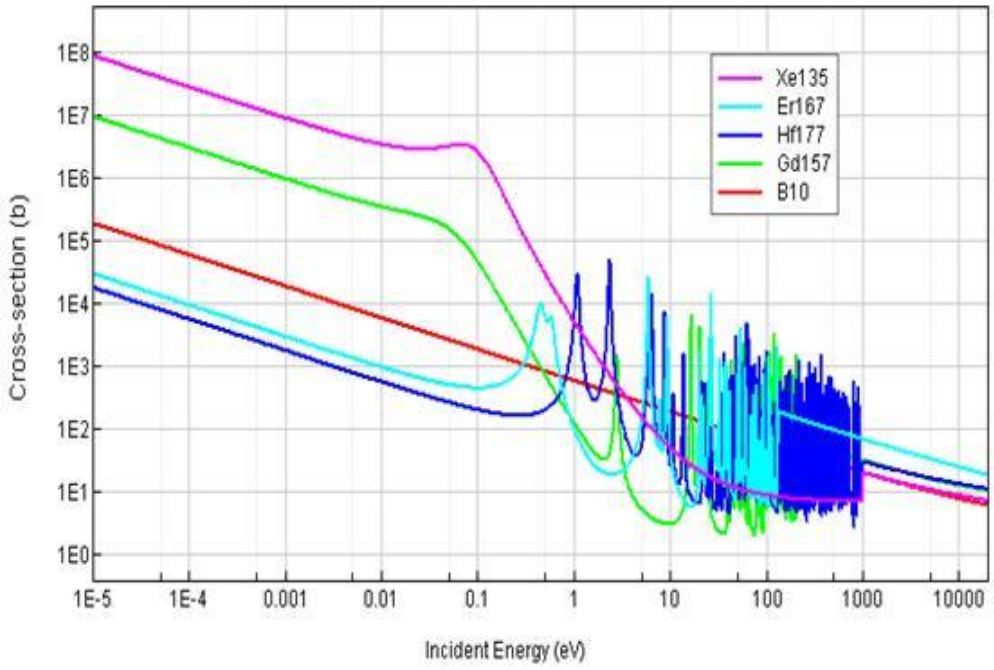

Figure 18. ^{167}Er, ^{135}Xe, ^{157}Gd, ^{10}B and ^{177}Hf Capture Cross Sections

Table 17. Effects on K_{eff} with Burnable Poison Doped Actinides

Burnable Absorber	**Mixture**	**K_{eff}**		
		^{242m}Am	**^{249}Cf**	**^{251}Cf**
^{167}Er	80% fuel, 20% absorber	1.544 ± 0.005	1.164 ± 0.001	1.487 ± 0.001
^{135}Xe		0.098 ± 0.004	0.049 ± 0.003	0.094 ± 0.004
^{157}Gd		0.564 ± 0.009	0.183 ± 0.005	0.479 ± 0.008
^{10}B		1.467 (± 0.001	0.974 ± 0.001	1.392 ± 0.001
^{177}Hf		1.562 (± 0.001	1.217 ± 0.001	1.518 ± 0.001

CHAPTER IV

DEEP SPACE MISSION COMPATIBILITY

New Horizons, launched on 19 January 2006, is a spacecraft designed to explore the Pluto system, including Pluto satellites Charon, Nix and Hydra [37]. Mission travel time to Pluto is anticipated to take 10 years, powered by RTG units, with additional power to arrive at Kuiper Belt Objects (KBO) approximately 5 years later [37].

IV.A. Deep Space Missions and the FFMCR Using Advanced Actinide Fuels

Recent literature suggests FFMCR propulsion capabilities shown in Table 18 [23]. GRAVASIST, a private computational orbital trajectory code, is used in this work to determine delta-V (the total change in velocity required to capture certain orbits, accelerate or decelerate) requirements for multiple scenarios.

Table 18. Potential Propulsion Capabilities Utilizing the FFMCR Concept

Propulsion Capability	
Velocity	0.1c
Force	1.4 N
Operation	Continuous
Duration	4 years (at 10MW)

Orbital trajectory graphical data is determined by the Satellite Tool Kit (STK). STK is a COTS (Commercial-Off-The-Shelf) physics-based software engine that displays and analyzes space objects in real or simulated time environments [38]. Data obtained from GRAVASIST is used as input to STK and trajectory visualization produced.

Right ascension is a celestial coordinate used to measure longitude on the celestial sphere. Right ascension can also be defined as the angular distance measured eastward from the vernal equinox along the celestial equator. Declination is the celestial coordinate used to measure latitude above or below the celestial equator on the celestial sphere. Table 19 and 20 give the computed entry conditions upon arrival at Charon. The data indicates that, while a larger v-infinity is needed to accomplish less travel time between Earth and Charon, for g-tolerant payloads significantly shorter transients can be realized using the FFMCR concept with higher order actinides.

Table 19. Orbital Trajectory Data Set 1:
10, 15 and 20 Year Travel Times

Flight Duration (years)	Computed Parameter	Earth departure conditions	Charon arrival conditions
10	V-infinity (km/s)	18.37	10.84
	Declination (°)	-62.06	4.20
	Right Ascension	60.91	184.58
15	V-infinity (km/s)	10.95	9.66
	Declination (°)	-62.01	7.68
	Right Ascension	59.08	180.92
20	V-infinity (km/s)	7.37	9.46
	Declination (°)	-62.68	8.56
	Right Ascension	58.68	180.31

Table 20. Orbital Trajectory Data Set 2:
3, 6 and 9 Year Travel Times

Flight Duration (years)	Computed Parameter	Earth departure conditions	Charon arrival conditions
3	V-infinity (km/s)	40.03	52.31
	Declination (°)	-20.82	-58.98
	Right Ascension	302.02	118.38
6	V-infinity (km/s)	21.68	24.96
	Declination (°)	-22.66	-58.19
	Right Ascension	295.33	119.83
9	V-infinity (km/s)	17.35	15.84
	Declination (°)	-23.74	-57.44
	Right Ascension	291.12	121.50

IV.B. Conceptual Implementation of FFMCR for Micro Payloads

Practical implementation of the FFMCR concept utilizing higher actinides may be accomplished using state-of-the-art material, nanotechnology, compact pulsed power, superconducting magnets and other COTS components. One example of how fission fragment particles can be deployed for propulsion is shown in Figure 19. In this concept, the FFMCR is oriented horizontally with high energy fission fragments born in the bottom of the vehicle. Ions created in the core are focused and collimated by magnetic field lines using superconducting magnets. Bidirectional ions are guided through 90° sector magnets toward exit collectors. High energy fission fragments are finally directed out the bottom of the spacecraft to create very high specific impulses at very high efficiency. Radiation protection is accomplished using a thin layer of lightweight neutron, gamma and ion attenuation material. Deep space and interstellar mission scenarios may require separation of the payload bay from the entire FFMCR subsystem, which may be executed using a separation ring mechanism similar to existing spacecraft. Advanced light weight nano metamaterials may be applied to the outer cone region for extreme deep space protection from micrometeroids.

It is acknowledged that the spacecraft concept proposed in this work (Figure 19) relies on multiple low technical readiness level (TRL) technologies, which increases developmental risks; however, the concept of using the fission fragment reactor for propulsion is demonstrated.

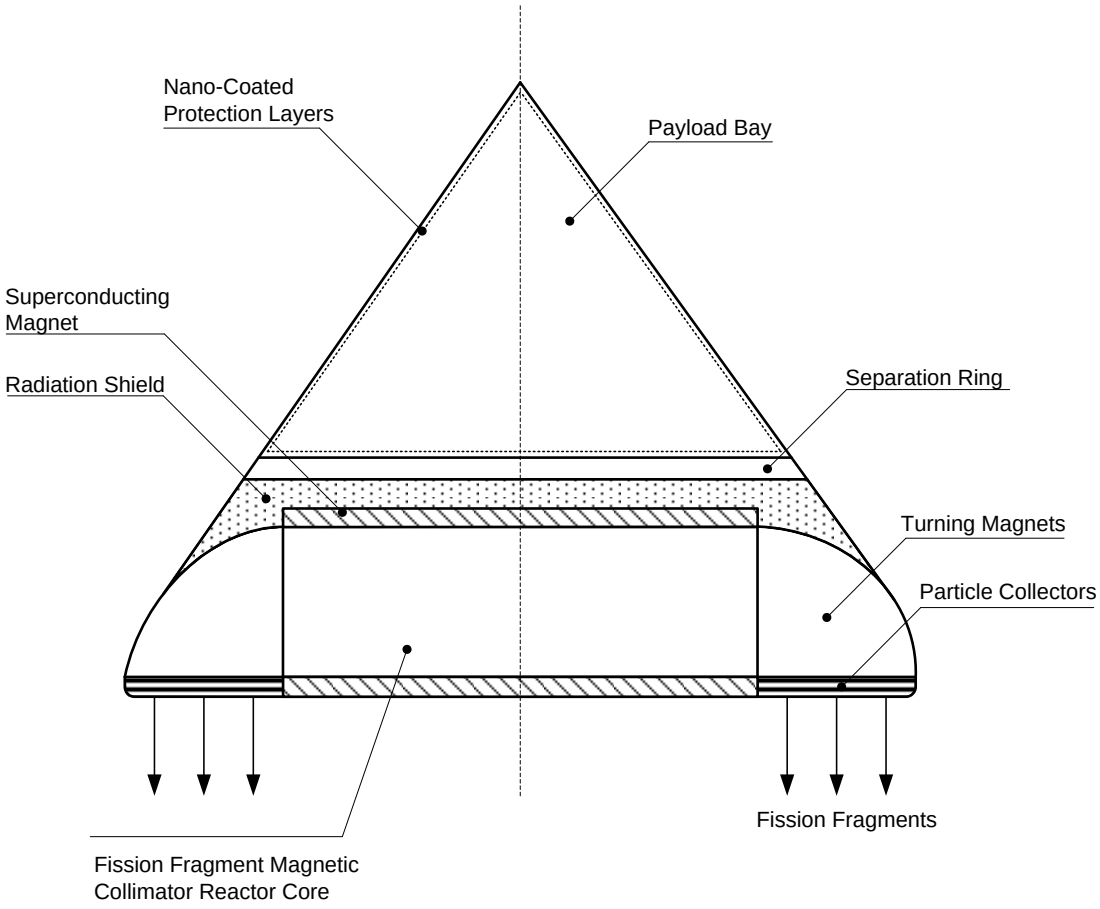

Figure 19. Conceptual Implementation of FFMCR with Advanced Actinide Core

CHAPTER V

CONCLUSIONS

V.A. Summary

High reliability-demanding applications, including deep space missions, require advanced power and propulsion sources. Ambitious goals, such as interstellar precursor missions beyond 200 astronomical units in 20 years, and 60-day round trip Mars missions, will require velocities on the order of 100 to 1,000 km/s, which are a factor of 10 – 100 greater than current exploration capabilities.

The fission fragment magnetic collimator reactor concept presented in this thesis, utilizing higher actinides, has properties conducive to high-reliability applications. The meta-stable isomer ^{242m}Am, coated on graphite fibers, is found to have superior properties (relative to uranium and plutonium baseline isotopes), which when combined with magnetic collimation may provide a novel solution in high-reliability demanding environments. Key advantages of using ^{242m}Am are summarized below.

- ^{242m}Am has a half-life of 141 years (applicable to most mission profile requirements).
- ^{242m}Am has a low specific activity of 9.8 Ci/g (for improved radiological safety) and low specific power of 0.002 W/g (for practical material integration).

- The ^{242m}Am actinide has one of the highest known thermal fission cross sections and produces a high neutron yield per neutron absorbed.
- The fission fragment kinetic energy of ^{242m}Am is approximately 10-15 MeV above baseline uranium and plutonium fragments.
- Prompt neutron and γ-ray emission is lowest for ^{242m}Am, potentially adding addition safety margins relative to uranium or plutonium.
- Heavy ion fragments appear to be controllable using voltages greater than 5 MV.
- A 1-2 micron thick ^{242m}Am fuel layer allows most fission fragments to escape for magnetic focusing.
- Three-dimensional Monte Carlo analysis of baseline and higher actinides indicates that, given the FFMCR configuration in this work, criticality can be achieved using ^{242m}Am, ^{249}Cf, and ^{251}Cf. System criticality is not achievable for ^{235}U, ^{239}Pu or ^{241}Pu.
- Burnable absorbers can be mixed with higher actinides to reduce criticality at high fuel loadings, with the largest effect due to ^{135}Xe and ^{157}Gd.
- Limited production and availability of ^{242m}Am reduces its potential as a fuel for power and propulsion; however, it is recognized that select plutonium isotopes suffer from similar production and availability limitations.

V.B. Recommendations

Americium-242m is clearly established as a promising fuel for reliability-demanding applications, and ^{249}Cf and ^{251}Cf isotopes appear to hold similar promising properties such as high neutron yield, low specific activities, large fission fragment masses and applicable radioactive half-life. Recommendations for future work include:

- Detailed analysis of higher actinide fuels such as ^{249}Cf and ^{251}Cf to quantify potential benefits when used in propulsion or power applications.
- Proof-of-principle experimental nanofabrication of ^{242m}Am, ^{249}Cf and ^{251}Cf fuels to examine commercialization and implementation viability.
- Studies to demonstrate experimental systems integration utilizing pulsed power, magnets and heavy ion beam focusing should be initiated or continued.

REFERENCES

1. L. LIOU, "Advanced Chemical Propulsion for Science Missions," NASA/TM-2008-215069, Glenn Research Center, Cleveland, Ohio (2008).

2. R. KIRKPATRICK, "Magnetized Target Fusion and Fusion Propulsion," Space Technology and Applications International Forum-STAIF, American Institute of Physics, Albuquerque, New Mexico (2002).

3. S. BOROWSKI, "Comparison of Fusion/Antiproton Propulsion Systems for Interplanetary Travel," NASA/TM 107030, Lewis Research Center, Cleveland, Ohio (1987).

4. M. EL-WAKIL, *Nuclear Energy Conversion*, American Nuclear Society, LaGrange Park, Illinois (1992).

5. S. GUNN, "Nuclear Propulsion – A Historical Perspective," Space Policy, **17**, 291 (2001).

6. F. DURHAM, "A Review of the Los Alamos Effort in the Development of Nuclear Rocket Propulsion," LA-UR-91-2295, *AIAA/NASA Conference on Advanced SEI Technologies*, Cleveland, Ohio (1991).

7. T. LAWRENCE, "Nuclear Thermal Rocket Propulsion Systems," IAA White Paper, International Academy of Aeronautics, Paris, France (2005).

8. R. JOHNSON, "Design, Ground Test and Flight Test of SNAP-10A First Reactor in Space," Atomics International, *Nuclear Engineering and Design*, **5**, 7-21 (1967).

9. M. EL-GENK, "Deployment History and Design Considerations for Space Reactor Power Systems," *Acta Astronautica*, **64**, 833 (2009).

10. J. BENNETT, *The Cosmic Perspective*, Addison-Wesley, San Francisco, California, (2002).

11. P. SCHMITZ, "Feasibility Study of a Nuclear-Stirling Power Plant for the Jupiter Icy Moons Orbiter," Space Technology and Applications International Forum – STAIF, Albuquerque, New Mexico (2005).

12. R. DANCHIK, *An Overview of Transit Development*, Johns Hopkins APL Technical Digest, **19**, 18 (1998).

13. D. KUSNIERKIEWICZ, "A description of the Pluto-bound New Horizons Spacecraft," *Acta Astronautica,* **57**, 135 (2005).

14. A. MARSHALL, *Space Nuclear Safety*, Krieger Publishing Company, Malabar, Florida (2008).

15. J. CHAN, "Development of Advanced Stirling Radioisotope Generator for Space Exploration," NASA/TM-2007-214806, NASA Glenn Research Center, Cleveland, Ohio (2007).

16. R. ABELSON, "Expanding Frontiers with Standard Radioisotope Power Systems," JPL/CALTECH, JPL D-28902, NASA Jet Propulsion Laboratory, Pasadena, California (2005).

17. J. FIX, *Astronomy: Journey to the Cosmic Frontier*, McGraw-Hill, Boston, Massachusetts (2001).

18. J. LAMARSH, *Introduction to Nuclear Engineering*, Prentice-Hall, Upper Saddle River, New Jersey (2001).

19. P. TSVETKOV, R. HART, T. PARISH, "Highly Efficient Power System Based on Direct Fission Fragment Energy Conversion Utilizing Magnetic Collimation," *Proceedings of the 11th International Conference on Nuclear Engineering (ICONE 11),* Tokyo, Japan (2003).

20. G. SAFONOV, "Direct Conversion of Fission to Electric Energy in Low Temperature Reactors," RM-1870, Science and Technology Program, RAND Corporation, Santa Monica, California (1957).

21. G. CHAPLINE, P. DICKSON, B. SCHTZLER, "Fission Fragment Rockets – a Potential Breakthrough," EGG-M-88285, Lawrence Livermore National Laboratory, California (1988).

22. Y. RONEN, E. SHWAGERAUS, "Ultra-thin 242Am Fuel Elements in Nuclear Reactors," *Nuclear Instruments and Methods in Physics Research A,* **455**, 442 (2000).

23. P. TSVETKOV, R. HART, D. KING, T. PARISH, "Planetary Surface Power and Interstellar Propulsion Using Fission Fragment Magnetic Collimator Reactor," *American Institute of Physics, Space Technology and Applications Forum-STAIF, Albuquerque, New Mexico,* **813**, 803 *(*2006).

24. P. TSVETKOV, "Direct Fission Fragment Energy Conversion Utilizing Magnetic Collimation," Ph.D. Dissertation, Texas A&M University, College Station, Texas (2002).

25. NASA, "Fission Surface Power System Technology for NASA Exploration Missions," http://www.ne.doe.gov (2008).

26. "ENDF/B-V1.6: The US Evaluated Nuclear Data Library for Neutron Reaction Data", IAEA-NDS-100, International Atomic Energy Agency, Vienna, Austria (1995).

27. P. NAGEL, *JANIS 1.0 User's Guide*, OECD-AEN/NEA-JANIS-1.0, NEA Data Bank, OECD Nuclear Energy Agency, Issy-les-Moulineaus, France (2001).

28. G. ROCHAU, "Charge, Mass, and Energy Distribution of Fission Fragments," Sandia National Laboratory, Internal Laboratory Report (2000).

29. J. Ziegler, "SRIM2000 The Stopping and Range of Ions in Matter," Monte Carlo computer program, http://www.srim.org/SRIM/SRIM%2008.pdf (2008).

30. SCALE5.0: A Modular Code System for Performing Standardized Computer Analysis for Licensing Evaluation, Radiation Safety Information Computational Center at Oak Ridge National Laboratory, Tennessee (2008).

31. R. Busch, "KENO V.a Primer: A Primer for Criticality Calculations with SCALE/KENO V.a Using GeeWiz," ORNL/TM-2005/135, Oak Ridge National Laboratory, Oak Ridge, Tennessee (2005).

32. N. GREENE, "BONAMI: Resonance Self-Shielding by the Bondarenko Method," ORNL/NUREG/CSD-2/V2/R5, RSIC/CCC-545, Oak Ridge National Laboratory, Oak Ridge, Tennessee (1997).

33. S. GOLUOGLU, "WORKER: Scale System Module for Creating and Modifying Working Format Libraries," ORNL/TM-2005/39, Oak Ridge National Laboratory, Oak Ridge, Tennessee (2005).

34. N. GREENE, "Users Guide for AMPX Utility Modules," ORNL/TM-2005/39, V6, Oak Ridge National Laboratory, Oak Ridge, Tennessee (2009).

35. M.L. WILLIAMS, "CENTRM: A One-Dimensional Neutron Transport Code for Computing Point Wise Energy Spectra," ORNL/TM-2005/39, V6, Oak Ridge National Laboratory, Oak Ridge, Tennessee (2009).

36. L. PETRIE, "KENOV.a: An Improved Monte Carlo Criticality Program," ORNL/TM 2005/39, Revision 6, Oak Ridge National Laboratory, Oak Ridge, Tennessee (2009).

37. D. KUSNIERKIEWICS, "A Description of the Pluto-Bound New Horizons Spacecraft," *Acta Astronautica,* **57**,136-137 (2005).

38. Analytical Graphics, Inc., STK, http://www.stk.com/, accessed on August 14, 2009

VITA

Troy Lamar Guy
2625 Bay Area Blvd, Houston, Texas 77058

Email: Troy.L.Guy@LMCO.com

Experience:

Lockheed Martin - Space Exploration and Science	2007-current
Lockheed Martin - Nevada Technologies	2000-2007
Lockheed Martin - Advanced Technologies	1999-2000

Education:

M.S. Nuclear Engineering, Texas A&M University, College Station, Texas, 2009

B.S. Electrical Engineering, University of Houston, Houston, Texas, 1998

Selected Contributed Publications and Presentations:

P.V. Tsvetkov, Guy, T.L. "Architectures Based on Direct Fission Fragment Energy Conversion for Interstellar Exploration," *Proceedings of Nuclear and Emerging Technologies for Space 2009*, Atlanta, Georgia (2009).

T.L. Guy, D. Hinshelwood, P. Corcoran, J. Douglas, V. Bailey, D.L. Johnson "Radiographic Driver System Optimization Using BERTHA," *14th IEEE International Pulsed Power Conference*, Dallas, Texas (2003).

V. L. Bailey, D. L. Johnson, P. Corcoran, I. Smith, J. E. Maenchen, I. Molina, K. Hahn, D. Rovang, S. Portillo, B. V. Oliver, D. Rose, D. Welsh, D. Droemer, T. Guy, "Design of a High Impedance MITL for the RITS-3 Accelerator," *14th IEEE International Conference on Pulsed Power*, **1**, 399 (2003).

B.L. Freeman, J. Boydston, J. Ferguson, T. Guy, B. Lindeburg, A. Luginbill, and J. Rock, "Preliminary Neutron Scaling of the TAMU 460 kJ Plasma Focus," *IEEE Pulsed Power/Plasma Science Conference*, Las Vegas, Nevada (2001).

T. Guy, B. Freeman, "Studies to Improve Performance of Maxwell ATLAS Rail-Gap Switches," *27th IEEE International Conference on Plasma Science*, New Orleans, Louisiana (2000).